Water Regulation in Cyanobacterial Biocrusts from Drylands: Negative Impacts of Anthropogenic Disturbance

Yolanda Cantón [1,2,*], **Sonia Chamizo** [1,2], **Emilio Rodriguez-Caballero** [1,2], **Roberto Lázaro** [3], **Beatriz Roncero-Ramos** [1], **José Raúl Román** [1] **and Albert Solé-Benet** [3]

[1] Department of Agronomy, University of Almeria, Carretera de Sacramento sn., La Cañada de San Urbano, 04120 Almeria, Spain; scd394@ual.es (S.C.); rce959@ual.es (E.R.-C.); brr275@ual.es (B.R.-R.); jrf979@ual.es (J.R.R.)

[2] Research Centre for Scientific Collections from the University of Almería (CECOUAL), Carretera de Sacramento sn., La Cañada de San Urbano, 04120 Almeria, Spain

[3] Experimental Station of Arid Zones, CSIC, Carretera de Sacramento sn., La Cañada de San Urbano, 04120 Almeria, Spain; lazaro@eeza.csic.es (R.L.); albert@eeza.csic.es (A.S.-B.)

* Correspondence: ycanton@ual.es

Abstract: Arid and semi-arid ecosystems are characterized by patchy vegetation and variable resource availability. The interplant spaces of these ecosystems are very often covered by cyanobacteria-dominated biocrusts, which are the primary colonizers of terrestrial ecosystems and key in facilitating the succession of other biocrust organisms and plants. Cyanobacterial biocrusts regulate the horizontal and vertical fluxes of water, carbon and nutrients into and from the soil and play crucial hydrological, geomorphological and ecological roles in these ecosystems. In this paper, we analyze the influence of cyanobacterial biocrusts on water balance components (infiltration-runoff, evaporation, soil moisture and non-rainfall water inputs (NRWIs)) in representative semiarid ecosystems in southeastern Spain. The influence of cyanobacterial biocrusts, in two stages of their development, on runoff-infiltration was studied by rainfall simulation and in field plots under natural rainfall at different spatial scales. Results showed that cover, exopolysaccharide content, roughness, organic carbon, total nitrogen, available water holding capacity, aggregate stability, and other properties increased with the development of the cyanobacterial biocrust. Due to the effects on these soil properties, runoff generation was lower in well-developed than in incipient-cyanobacterial biocrusts under both simulated and natural rainfall and on different spatial scales. Runoff yield decreased at coarser spatial scales due to re-infiltration along the hillslope, thus decreasing hydrological connectivity. Soil moisture monitoring at 0.03 m depth revealed higher moisture content and slower soil water loss in plots covered by cyanobacterial biocrusts compared to bare soils. Non-rainfall water inputs were also higher under well-developed cyanobacterial biocrusts than in bare soils. Disturbance of cyanobacterial biocrusts seriously affected the water balance by increasing runoff, decreasing soil moisture and accelerating soil water loss, at the same time that led to a very significant increase in sediment yield. The recovery of biocrust cover after disturbance can be relatively fast, but its growth rate is strongly conditioned by microclimate. The results of this paper show the important influence of cyanobacterial biocrust in modulating the different processes supporting the capacity of these ecosystems to provide key services such as water regulation or erosion control, and also the important impacts of their anthropic disturbance.

Keywords: biological soil crust; arid; runoff; infiltration; soil water balance; dew

1. Introduction

The ability of biological soil crusts or biocrusts to survive in water-limited environments has made them a component of major interest in drylands. Biocrusts are widely distributed communities [1] composed of cyanobacteria, algae, lichens and mosses, living within the uppermost part of the soil together with heterotrophic microorganisms such as bacteria and fungi [2,3]. Cyanobacteria are not only an essential component of cyanobacteria-dominated biocrusts but also of lichen- and moss-dominated biocrusts in many ecosystems [4]. Indeed, cyanobacteria-dominated biocrusts are found in all biomes [5], living in a very diverse range of environments, thanks to the singular features they own that contribute to their broad success, such as: their capability to survive under extreme temperatures in the hottest and coldest climates [6,7]; their tolerance to desiccation and water stress [8] and to high saline environments [9]; their resistance against high levels of UV radiation [10]; their capability of photosynthetic CO_2 reduction even at very low concentrations of inorganic carbon; or the ability of many cyanobacterial species to fix N_2 [11,12].

Cyanobacteria are considered primary colonizers of terrestrial ecosystems [13] as well as important facilitators for the establishment of later organisms, such as mosses, lichens [14] and vascular plants [15,16]. Biocrust-forming cyanobacteria have been described as ecosystem engineers due to the multiple key ecosystem functions they play [17]. For example, it has been demonstrated that although cyanobacterial biocrusts show lower chlorophyll concentrations than vascular plants, they are the dominant primary producers in arid environments thanks to their ability to convert soil moisture and non-rainfall water contributions into useful resources by carbon fixation [17,18]. Moreover, N-fixing cyanobacteria increase soil nitrogen content along with carbon, playing an important role in soil fertility in almost all types of ecosystems [19], but especially in the arid and semiarid ones, where nitrogen, after water, is the most important factor limiting net primary production and organic matter decomposition [20]. Furthermore, sticky cyanobacterial exopolysaccharide sheaths entrap and join soil particles, stabilizing the soil surface [21], promoting soil aggregate formation [22] and increasing soil resistance to water and wind erosion [23–28]. By conferring resistance to wind, cyanobacteria not only prevent soil loss but also long-range transport of soil particles and nutrients during wind storms, which has important implications on climate, productivity and human health [13].

Cyanobacteria, as a major component of biocrusts, also modify soil hydrology via different pathways. Biocrusts increase surface roughness and surface storage capacity, which in turn affect water residence time on the surface [29]. They also affect soil porosity, aggregation and organic matter content [30,31], which influence water movement and retention in soil at rates that depend on biocrust development and cover [32,33]. Thus, rougher late-developmental cyanobacterial biocrusts may significantly increase water infiltration into the soil compared to bare soils or incipient cyanobacterial biocrusts, especially in fine-textured soils [34]. Nevertheless, the infiltration rate in cyanobacterial biocrusts is lower than in vegetated patches [35], and they act as runoff sources when compared with vegetation. Thus, inhabiting the interplant spaces, biocrusts form a two-phase system in which runoff generated in biocrust patches is redistributed to vegetation, which act as a runoff sink [36–38]. This process of runoff generation and re-infiltration plays a crucial role in promoting overall ecosystem productivity, and modulates the hydrological response at coarser scales [38]. For all these reasons, the influence of biocrusts, in general, and cyanobacterial biocrusts in particular, on runoff and infiltration has received considerable attention during the last two decades [39–43]. However, the influence of cyanobacterial biocrusts on other critical components of the water balance, such as soil moisture and evaporation [44–49] has been less studied, and it is even less known how they can affect non-rainfall water inputs (NRWIs) including water absorption, dew and fog. Moreover, it is of special importance to know how increasing anthropic activities in arid and semiarid ecosystems such as the expansion of agriculture, animal grazing, and recreational activities may impact cyanobacterial biocrust communities and their capacity to provide key water regulation services to society. All these activities disrupt cyanobacterial biocrusts, reduce their proportion within the whole microbiome [50] and change the cyanobacterial community composition by decreasing the abundance of diazotrophic

species (such as *Nostoc* spp. or *Scytonema* spp.), and replacing them by other species which usually dominate early-successional biocrusts (e.g., *Microcoleus* spp.) [51,52]. Such disturbances may also entail important changes in the role of cyanobacterial biocrusts in hydrological and biogeochemical processes and erosion [42,43,53,54]. As a result, vital ecological functions in drylands will be lessened, leading to the loss or decline in their capacity to provide services to society.

The integrated analysis of the influence of cyanobacterial biocrusts on infiltration-runoff, evaporation, soil moisture and NRWIs, is necessary to elucidate their role in the water balance and provide insight on their contribution to dryland ecosystems capacity for soil water regulation. Due to their vulnerability to physical anthropic disturbance, and considering the growing human activity in dryland regions, the impact of such common disturbances on the water balance components should be also studied. The aims of this paper are, therefore, to analyze the influence of cyanobacterial biocrusts in the processes driving soil water regulation and erosion, and to understand how disturbance will affect this influence, in two semiarid ecosystems with contrasting soil texture. Our specific goals are to: (1) analyze the influence of cyanobacterial biocrusts on infiltration-runoff at different spatial scales and on erosion; (2) examine the effect of cyanobacterial biocrusts on soil moisture, soil evaporation and NRWIs; (3) evaluate how the disturbance of the cyanobacterial biocrust affects the water balance components and erosion; and (4) to characterize the dynamics of cyanobacteria recolonization after their removal.

2. Material and Methods

2.1. Study Sites

Two semiarid sites were selected in the province of Almería located in southeastern Spain (Figure 1). They are both representative of the most common cyanobacterial biocrust habitats and spatial distribution in semiarid areas, but are characterized by contrasting lithologies and soil textures.

(i) El Cautivo (37°00′37″ N, 2°26′30″ W) is located in the Tabernas Basin, a badlands surrounded by the Alhamilla, Filabres, Nevada and Gador Mountain Ranges. The climate is semiarid thermo-Mediterranean, characterized by hot, dry summers and mild temperatures the rest of the year, with rain falling mostly in winter. Mean annual rainfall is 235 mm and the annual potential evapotranspiration is around 1500 mm, indicating a high water deficit. The mean annual temperature is 17.9 °C (with an absolute maximum of 45 °C and minimum of −4.5 °C) [55]. The basin is mainly filled with calcaric–gypsiferous mudstone and calcareous sandstone. Soil texture is silty loam (~60% silt). The landscape is formed by NW–SE valleys where North to East-facing slopes (with gradients of about 30°) have incipient soils (Endoleptic Regosols and Lithic-xeric Torriorthent) and are densely covered (often over 70% of the soil surface) with lichen-dominated biocrusts (*D. diacapsis* (Ach.) Lumbsch, *Squamarina lentigera* (Web) Poelt, *Lepraria isidiata* Llimona and *Buellia zoharii*), cyanobacteria and mosses, the last in much lower proportions. At the pediment, on gentle slope gradients, Haplic Calcisols or Xeric Haplocalcid soils are relatively thick. They are covered by very scattered annual (around 9%) and perennial plants (*Stipa capensis* Thunb., *Helianthemun almeriense* Pau, *Hammada articulate* (Moq.) O. Bolós and Vigo, *Artemisia barrelieri* Besser, *Salsola genistoides* Poiret) and biocrusts (mainly cyanobacterial biocrusts) which are occupying interplant spaces, all together covering around 36% of the soil surface. The steeper south-west-facing slopes have slope gradients around 50° (and up to 70°) and they are eroded and much less stable than the rest of landforms. These SW facing hillslopes have poorly developed soils (Epileptic Regosols or Lithic Torriorthent), and scarce perennial (*S. genistoides* Poiret) or annual plant cover (*Moricandia foetida* Bourgeau ex Cosson), all together covering less than 5% of the soil surface [55,56]. There are cyanobacterial biocrusts on the more stable microsites (pediments), including lichens, such as *Endocarpon pusillum*, *Fulgensia fulgida* (Nyl.) Szatala), *Fulgensia* spp and *Collema* spp.
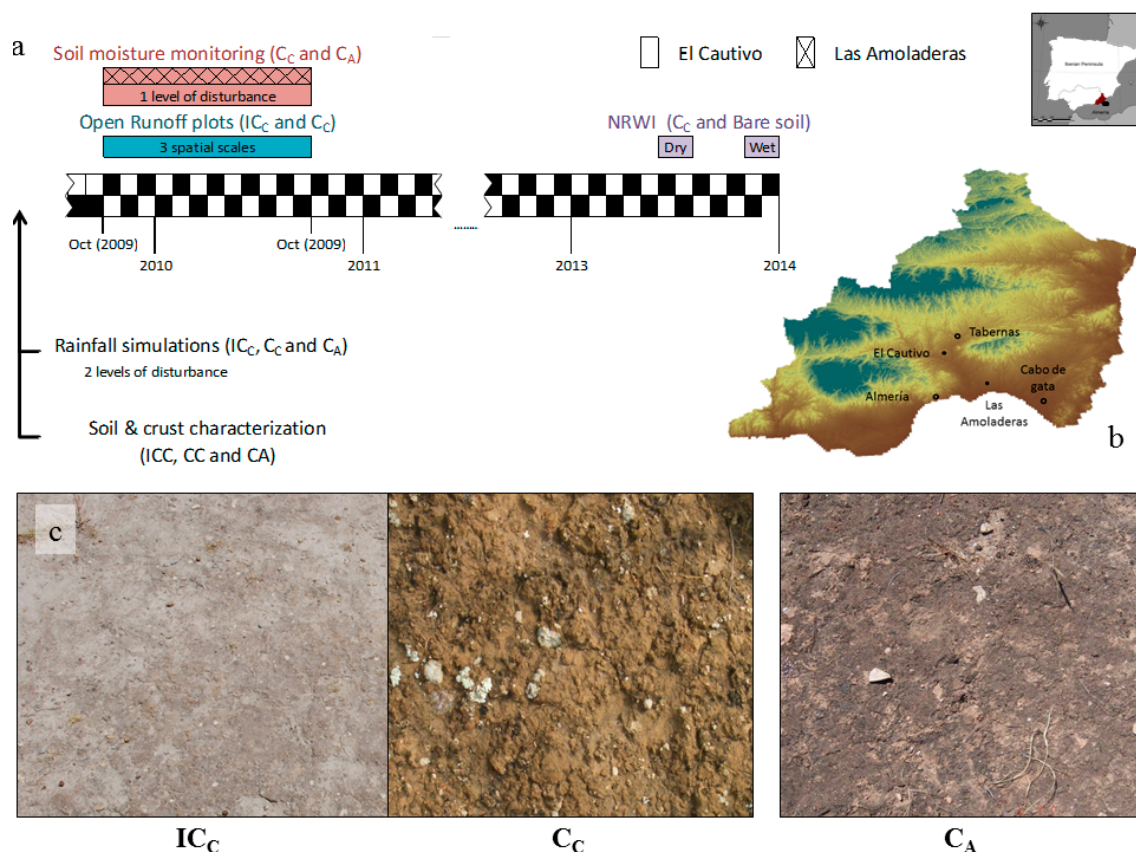
Figure 1. Sampling and monitoring schedule (**a**); location of the study sites (**b**); photos of the cyanobacterial crust types (**c**): incipient-cyanobacteria (IC$_C$) and well-developed cyanobacteria (C$_C$) at El Cautivo, and well-developed cyanobacteria at Las Amoladeras (C$_A$).

(ii) Las Amoladeras (36°48′34″ N, 2°16′6″ W) is a representative coastal-steppe ecosystem, located in the Cabo de Gata-Níjar Natural Park. It consists of an exposed and dissected caliche area in the flat part of an alluvial fan system. The climate is also semiarid thermo-Mediterranean. Summers are long and hot with infrequent and random rainfall events. Mean annual precipitation is 220 mm, with a severe interannual variation, and a mean annual temperature of approximately 18 °C. The annual potential evapotranspiration of approximately 1390 mm (nearby meteorological Station, Níjar) [57] reflects the strong water stress in this system. Soils, classified as Calcaric Leptosols and Haplic Calcisols, are thin with a sandy loam texture (~60% sand) and saturated in carbonates [31,32]. Vegetation is scarce and dominated mainly by *Macrochloa tenacissima* (L.) Kunth, but there are other relatively frequent dwarf shrubs such as *Thymus hyemalis* Lange, *Helianthemum almeriense*, *Sideritis pusilla* (Lange) Pau, *Hammada articulata*, *Lygeum spartum* L., *Salsola genistoides* Juss. ex Poir., and *Launaea lanifera* Pau. Perennial plant cover represents around 20% of the total ground cover and annual plants around 10%. Biocrusts (mainly lichens, cyanobacteria and mosses) occupy open areas among scattered shrubs and represent up to 30% of the soil surface. Among lichens, *Diploschistes diacapsis* is the most abundant. The rest of the area is stony with frequent rock outcrops [31].

Two types of cyanobacterial biocrusts were selected at El Cautivo and only one in Las Amoladeras. Based on previous studies [58,59], two cyanobacterial biocrust types were distinguished at El Cautivo: (a) a smooth, light-brown biocrust, macroscopically undifferentiated, with little cyanobacterial cover and/or biomass (hereafter incipient-cyanobacterial biocrust, IC$_C$) (Figure 1c, IC$_C$), and (b) a rough or slightly rough dark-brown biocrust, with high cyanobacterial cover and biomass, including also some pioneer lichens such as *Endocarpon pusillum*, *Fulgensia* spp or *Collema* spp (hereafter well-developed cyanobacterial biocrust, C$_C$) (Figure 1c, C$_C$). These crusts are composed by several bacterial

phyla such as: Proteobacteria, Actinobacteria, Bacteoidetes, Acidobacteria, Cyanobacteria and Verrucomicrobia [60]. Büdel et al. [61] found 14 cyanobacterial genera, being the most abundant ones: *Nostoc*, *Leptolyngbya*, *Scytonema* and *Phormidium*. Some filamentous cyanobacteria have been also identified, to the species level, such as: the heterocystous cyanobacteria, *Tolypothrix distorta* and *Scytonema hyalinum*; and the non-heterocystous *Leptolyngbya frigida*, *Microcoleus steenstrupii* and *Trichocoleus desertorum* [62].

In Las Amoladeras, only the dark well-developed cyanobacterial biocrust was frequent, and appeared covering a significant area of the soil surface (hereafter C_A) (Figure 1c, C_A), while the incipient-cyanobacterial biocrust appeared in very small patches and was not included in this study. These biocrusts have been characterized by [63], showing that their cyanobacterial community was dominated by the bundle-forming *Microcoleus* sp. and the unicelular *Chroococcidiopsis* sp. Other filamentous nonheterocystous species composing the biocrusts were *M. steenstrupii*, *Oculatella kazantipica*, *Schizothrix* cf. *calcicola* and other Oscillatoriales. The heterocystous species identified by these authors were *Nostoc commune*, *Scytonema hyalinum*, *Tolypothrix distorta*, and *Nostoc calcicola*.

2.2. Cyanobacterial Biocrusts and Underlying Soils Sampling and Measurements

In summer 2009 we identified four representative areas covered by cyanobacteria-dominated biocrusts (C_A) at Las Amoladeras, and eight representative areas at El Cautivo, covered by ICc (4) and Cc (4), separated 10–100 m from each other and located over the same landform and soil type (hereafter "sampling areas"). In order to characterize these cyanobacterial biocrust types, selected a priori, and their influence on soil hydrological properties, a representative plot of 0.5×0.5 m was identified within each sampling area and the following measurements were performed: (i) Biocrust roughness, measured by scanning soil surface with a Leica ScanStation 2 terrestrial laser scanner (Leica Geosystems AG, Heerbrugg, Switzerland). From the laser scanner point clouds recorded on the plots, two different micro-topographic indices were calculated for each plot: (a) surface storage capacity (SSC), defined as the amount of water that can be stored in the soil surface micro-depressions of each plot and (b) random roughness following the methodology proposed by [29]. (ii) Cyanobacterial biocrust cover, by analyzing images of the biocrusts (taken with a digital camera CANON EOS 600D) and applying support vector machine classification. (iii) In addition, biocrust reflectance was acquired around solar noon (12–16 h local time) under clear sky conditions with a GER2600 portable spectroradiometer (Spectra Vista corporation, Poueghkeepsie, New York, USA). Based on these data, we calculated two indices related with cyanobacterial biocrust development: the albedo of the surface in the VIS region (400–700 nm) and chlorophyll *a* spectral absorption feature. Surface albedo was calculated as the square root of the sum of the squares of reflectance at every wavelength between 400 and 700 nm. The chlorophyll *a* spectral absorption was calculated as the value of the continuum-removed spectra at 680 nm [64]. Continuum removal values lower than 1.0 indicate absorption peaks.

After the above mentioned measurements, one sample was collected from each plot (0–0.5 cm deep, surface layer) as well as the soil underneath them (1 cm depth, i.e., 0.5–1.5 cm soil layer). The samples were transported in isothermal bags to the laboratory, where they were dried, crushed with a roller and grounded with a mechanical agate mortar and stored at 4 °C in dark conditions until the analyses. These samples were used to determine the following properties: exopolysaccharide (EPS) and chlorophyll *a* content of the biocrust; total organic carbon and nitrogen content of the biocrust and the underlying soil; and available water capacity and aggregate stability of the underlying soil. EPSs were recovered using three extractions with Na_2EDTA 0.1 M [65] and then quantified using the phenol-sulfuric acid assay [66]. The absorbance of the supernatant was measured at 488 nm in a spectrophotometer and the EPS concentration was obtained from a calibration curve built with known concentrations of glucose. Chlorophyll *a* concentration was extracted by hot ethanol (70 °C, 5 min) neutralized with a small amount of $MgCO_3$ (0.1% w/v) in sealed test tubes and then vortexed [67].

Samples were centrifuged, and the absorbance of the supernatant was measured in a spectrophotometer at 665 nm. Chlorophyll *a* concentration was calculated according to the equation by [68] (Equation (1)):

$$\text{Chlorophyll } a \text{ (µg g soil}^{-1}) = (11.9035 \times A \text{ (665} - 750) \times V)/\text{g soil}^{-1} \times L \tag{1}$$

where *A* is the absorbance value at the specific wavelength, *V* is the volume of the solvent (mL) and *L* is the optical path length of the spectrophotometer cuvette.

Total organic carbon content was determined by oxidation with sulfuric acid and potassium dichromate, and later measurement of the absorbance in a spectrophotometer at 590 nm [69]. Total nitrogen was measured by the Kjeldhal method [70]. Total soil available water holding capacity was determined as the difference between water holding capacity at field capacity (−33 kPa) and at the wilting point (−1500 kPa), both measured with the Richard's pressure-membrane extractor. Soil aggregate stability of 4–5 mm aggregates was determined with the drop test [71], using 40 soil aggregates under each crust type. Finally, hydraulic conductivity (ks) was calculated for both cyanobacterial biocrusts at El Cautivo (ICc and Cc) using a minidisk tension infiltrometer with −0.5 cm pressure head (Decagon, Pullman, WA, USA), according to the method proposed by [72]

2.3. Measurement of Soil Surface Hydrological Processes

Water loss by runoff was measured under both simulated rainfall (to reproduce an extreme rainfall event) and natural rainfall conditions (as biocrust hydrological response was expected to depend on rainfall properties and antecedent moisture conditions):

(a) Rainfall simulation experiments were conducted in both study sites to examine the influence of cyanobacterial biocrusts and their disturbance on infiltration-runoff and water erosion under an extreme rainfall at plot scale. On each sampling area and adjacent to the sampling plots described in Section 2.2, four triads of 0.25 m^2 plots, close runoff plots, were installed per crust type (IC$_C$, C$_C$ and C$_A$). In each triad, one plot was left undisturbed, the crust was scraped off in another, and in the third, the crust was boot-trampled, treading on the plot 100 times (five rounds and 20 steps per round). One month after plots installation, a rainfall simulation (50 mm h^{-1} during 1 hour) was carried out on each plot using the rainfall simulator designed by [73]. During rainfall simulation, runoff volume was measured with a test tube at set intervals throughout the simulation experiment and sediment yield was estimated from runoff samples collected at fixed intervals of 15 minutes.

(b) In addition, at El Cautivo, runoff was measured during the hydrological year 2009–2010 (October 2009–September 2010) in open plots located in the sampling areas (Section 2.2). We selected three of the four sampling areas dominated by well-developed cyanobacterial biocrusts and runoff was measured on 3 different sets of open runoff plots, under natural rainfall conditions: (i) the first set consisted of six about 1 × 1 m open runoff plots, three on soil with well-developed cyanobacterial biocrusts (C$_C$) and three on soil where the biocrust was removed in 2007 and has remained unaltered since then, allowing recolonization by cyanobacteria. These plots showed an incipient cyanobacterial biocrust (IC$_C$) during the study period; (ii) the second set was formed by four 7 to 10 m^2 open small-hillslope plots, two on well-developed cyanobacterial biocrusts (C$_C$), and the other two on soil where incipient cyanobacterial biocrusts (IC$_C$) had recolonized, after cyanobacterial crust removal in 2007 as mentioned above; (iii) and the third set consisted of two about 20 m^2 open hillslope plots covered by well-developed cyanobacterial crusts (C$_C$). In order to get comparable results, all the plots were set up on the same landform and soil type and next to the triads of runoff plots used for rainfall simulation. The smallest plots (first set), located at the top of gentle hillslopes and about 1 m from the watershed, were connected by a hose to a 20 L deposit. Total runoff in these plots was measured manually after each rainfall event between October 2009–September 2010. The larger plots (second and third sets) were connected to a 50 L tank equipped with a 0.5 L tipping-bucket rain gauge connected to a data logger that stored data for the same period. Surface storage capacity (SSC) was calculated for each plot of the three sets.

In both study sites, we also monitored soil moisture in soils covered by well-developed cyanobacterial biocrusts and bare soils. To do this, we selected three of the four sampling areas dominated by well-developed cyanobacterial biocrusts at each study site (C_A and C_C) (Section 2.2). On each of these sampling areas, we installed a pair of plots, consisting of a well-developed cyanobacterial biocrust and bare soil from which the cyanobacterial biocrust was scraped off. Soil moisture was continuously monitored in all plots during one hydrological year (October 2009–September 2010) at a depth of 3 and 10 cm with EC-5 and 10 HS moisture probes, respectively (Decagon Devices, Inc., Pullman, Washington), and stored every 10 min in Decagon Em50 data loggers. Complete dataset was divided in different drying periods or drying events, defined as periods with no rain during ten consecutive days. A total of 8 and 5 drying events were analyzed at El Cautivo and Las Amoladeras, respectively.

Finally, as NRWIs may comprise a significant proportion of the total annual precipitation in many dry ecosystems, we measured NRWIs at El Cautivo during a dry soil period (June and July 2013) and a wet soil period (November and December 2013) using six automated microlysimeters (15 cm diameter × 9 cm depth) [74], three containing C_C and three bare soil (biocrust-scraped soil). Samples were collected from three of the four sampling areas dominated by well-developed cyanobacterial biocrust (C_C) (Section 2.2). On each area, a pair of microlysimeters were inserted into the soil, and then carefully removed [74]. The biocrust was scraped from one of the two microlysimeters once they were extracted from the soil. The automated microlysimiter consisted of a 3 kg rated capacity single-point aluminum load cell (model 1022, 0.013 × 0.0026 × 0.0022 m, Vishay Tedea-Huntleigh, Switzerland), which was connected to a datalogger (CR1000, Campbell Scientific, Logan, UT, USA) that stored data every 15 minutes. The load cell gave an mV signal, so that the datalogger registered the ratio of the load cell mV signal to the input voltage (mV V^{-1}). To transform voltage to weight, we performed a calibration of the load cell by adding loads with increasing weight.

Both study sites were equipped with a weather station that stored microclimate data every 30 minutes during the study periods. Rainfall was recorded by a tipping-bucket gauge with a 0.20 mm resolution located close to the sampling areas.

Figure 1 shows the different measurement settings and sampling date periods. In general, the number of replicates in our experimental design was constrained by the need of avoiding as much as possible the disturbance caused by trampling during plots setting, especially for installing runoff plots at hillslope scale, and also the difficulty of finding homogeneous areas (biocrust cover, soil properties, topography etc.), particularly when selecting large plots in ecosystems with high ground cover and topographic heterogeneity. Despite the limited number of replicates in space, our experimental design allowed a high number of replicates in time (high number of events).

2.4. Biocrust Successional Dynamics after Disturbance

To explore how long could persist the influence of cyanobacterial biocrust disturbance on surface hydrology, we analyzed the natural recovery of this biocrust after disturbance. To do this, we monitored biocrust cover and species recovery after removal of the well-developed cyanobacterial biocrusts in three plots at El Cautivo site for two years. In each plot the cyanobacterial biocrust was carefully removed from a 30 × 30 cm area and a quadrat grid with 36 cells (5 × 5 cm each cell) was used for in-situ inventories after 12 and 24 months from biocrust removal. Cyanobacterial biocrust cover in each grid cell as well as mosses and every lichen species were visually estimated in mm^2. Young light and dark lichen thalli (too small to allow species identification) were recorded as species. The number of grid cells in which each species or biocrust type appeared was recorded as the frequency of that species and the Shannon–Weaver biodiversity index was calculated for every plot and year.

2.5. Data Analyses

Previous to the statistical analyses, all data were checked for normality assumptions. Significant differences in surface physicochemical properties among the three cyanobacterial biocrust types (ICc and C_C at El Cautivo and C_A from Las Amoladeras) were explored by means of One-Way Anova and the Fisher's post-hoc test. Water gains by NRWIs during the different NRWI events occurred in the dry and wet soil periods were calculated as the difference in weight between the night-time maximum and the minimum of the day before [74]. Using these data, we explored differences in water gains by NRWIs between cyanobacteria-dominated biocrusts and bare soil at El Cautivo by means of General Linear Mixed Models (LMMs), using soil cover as a fixed factor and event as a random categorical predictor. To quantify water losses by runoff, we calculated runoff rates (L m^{-2}) during both, the rainfall simulation experiments at the two study sites, and natural rainfalls at El Cautivo site. The effect of biocrust disturbance on runoff and sediment yield measured during rainfall simulation experiments was analyzed using One-Way ANOVA and differences among undisturbed, trampled and removed biocrusts were further analyzed using the Fisher's test. Due to the limited number of replicates at hillslope scales, significant differences in runoff rates among the plot, small-hillslope and hillslope scales were analyzed using the student's T-test. The effect of soil cover (bare soil and well-developed cyanobacterial biocrust) on water losses by evaporation was also evaluated at the two study sites. To do this, we calculated soil water losses during drying events as the difference between actual volumetric water content (VWC) and maximum volumetric water content (VWCmax) after rainfall. In addition, we fitted each single drying event to a linear equation and used the slope (b) as a proxy of soil moisture decrease rate [75]. The influence of cyanobacterial biocrust on soil moisture decrease rate (b values) was explored by fitting a LMM with repeated measures, one on each study site, using soil cover as a fixed factor and event as a random categorical predictor. Finally, after checking the normality of the variables, one-Way Anova was applied to evaluate differences in cover and biodiversity between the two years of natural recovery of the cyanobacterial biocrust after its removal (Section 2.4). Moreover, Kruskal-Wallis analysis was performed to analyze the difference in rainfall properties (number of rainy days per month, total rainfall volume per month, monthly absolute maximums rainfall intensity, monthly mean of daily maximums of rainfall intensity and monthly mean of rainfall intensity) between the two years of natural recovery of the cyanobacterial biocrust. Statistical analyses were conducted using STATISTICA 8.0 (StatSoft, Inc., Tulsa, Oklahoma, USA.

3. Results

Most properties measured (roughness, EPS productivity, chlorophyll *a*, organic carbon, total nitrogen contents of the biocrust and the underlying soil as well as aggregate stability from the underlying soil) were significantly higher in well-developed (C_C at El Cautivo, and C_A at Las Amoladeras) than in incipient (IC$_C$) cyanobacterial biocrusts, supporting our identification of the crust types by developmental stage (Table 1). On the contrary, albedo was lower in C_C than in IC$_C$, coinciding with the darkening associated to higher cyanobacterial biocrust development [76,77]. In addition, C_C had higher soil available water holding capacity than IC$_C$, and the absorption peak at 680 nm, which is a good proxy of chlorophyll *a* content [77], was deeper in C_C than in IC$_C$. The well-developed cyanobacterial biocrusts at C_A were more similar to C_C than IC$_C$, although C_A showed some significant differences: lower surface roughness, higher chlorophyll *a* content, deeper spectral absorption at 680 nm and lower available water capacity in the soil underneath than C_C (Table 1).

Table 1. Characteristics of the cyanobacterial biocrust types and underlying soils. Different letters indicate significant differences between the three cyanobacterial biocrust types *(p < 0.05)*.

Crust/Soil Properties	El Cautivo		Las Amoladeras
	IC_C	C_C	C_A
Cyanobacteria cover (%)	33.3 ± 6.2b	80.3 ± 7.5a	73.1 ± 4.3a
Random roughness (cm)	3.9 ± 0.8b	8.7 ± 1.7a	4.2 ± 1.4b
Chlorophyll a content ($\mu g\ g^{-1}$)	2.3 ± 0.6c	5.3 ± 1.1b	7.4 ± 0.4a
EPS content ($mg\ g^{-1}$)	0.97 ± 0.39c	1.92 ± 0.05b	4.26 ± 0.37a
Crust organic carbon content ($g\ kg^{-1}$)	6.6 ± 1.3b	14.1 ± 5.7a	16.5 ± 3.1a
Total nitrogen content ($g\ kg^{-1}$)	1.0 ± 0.3b	1.7 ± 0.6a	1.8 ± 0.2a
Albedo (VIS region)	3.5 ± 0.3a	2.4 ± 0.5b	1.9 ± 0.8b
Absorption peak at 680 nm	0.94 ± 0.01a	0.87 ± 0.01b	0.77 ± 0.06c
Upper 1 cm soil organic carbon content ($g\ kg^{-1}$)	7.3 ± 1.0b	12.7 ± 2.1a	14.8 ± 3.2a
Upper 1 cm soil total nitrogen content ($g\ kg^{-1}$)	0.9 ± 0.2b	1.4 ± 0.3a	1.3 ± 0.4a
Upper 1 cm soil available water holding capacity (%)	15.7 ± 3.0b	21.8 ± 3.4a	14.5 ± 1.1b
Aggregate stability (number of drop impacts per aggregate)	20.5 ± 9.0b	45.8 ± 3.9a	49.3 ± 20.2a
Ks ($mm\ h^{-1}$)	5.7 ± 0.8b	12.7 ± 4.8a	

3.1. Effect of Cyanobacterial Biocrust on Soil Surface Hydrology

Cyanobacterial biocrusts affected the input of water from an inexhaustible source for the whole year, including dry periods, the NRWIs. The total water gained from NRWIs during dry-hot and cold-wet soil periods under well-developed cyanobacterial biocrusts and bare soils at El Cautivo is shown in Figure 2. A higher number of NRWI events was registered during the wet soil period (22 dew events during November and December 2013) than during the dry soil period (9 dew events during July and August 2013). The LMMs showed that both the event and soil cover had a significant effect on NRWI amount during both soil periods (see Table S1 in supplementary table). The total amount of NRWIs during the dry and wet soil period was 1.3 and 1.5 times higher in cyanobacterial biocrusts than in bare soils (Figure 2). A wider variability was found for NRWIs deposited on cyanobacterial biocrusts than on bare soils. Maximum NRWIs recorded during both periods was also higher on cyanobacterial biocrusts than on bare soils. Maximum NRWIs on cyanobacterial biocrusts was 0.28 and 0.31 mm, in dry and wet soil periods, respectively, and 0.22 and 0.23 mm in bare soils, respectively (Figure 2).
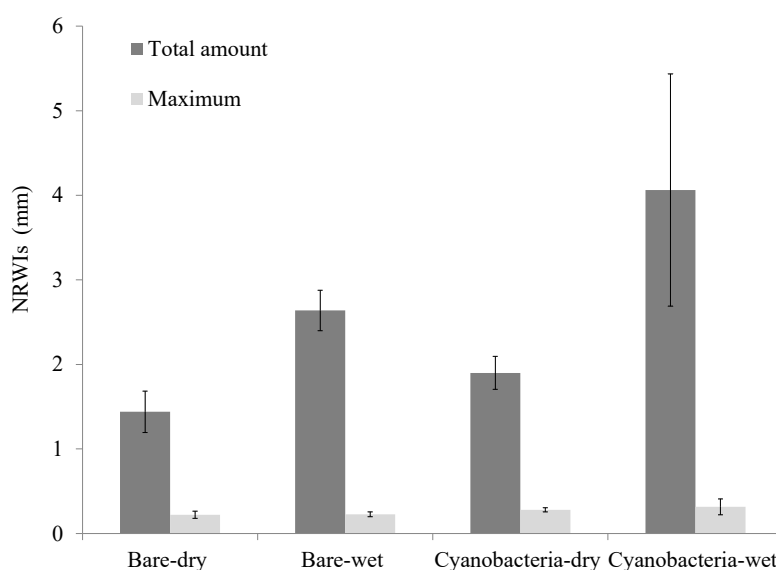

Figure 2. Total and maximum non-rainfall water inputs (NRWIs) amount in well-developed cyanobacterial biocrusts and bare soils at El Cautivo, during a dry (1 June–31 July 2013) and wet soil period (1 November–31 December 2013).

Concerning rainfall, during rainy periods, water gains in soils covered by cyanobacterial biocrusts were higher than in bare soils at both study sites. Figure 3 shows soil moisture content at a depth of 3 cm in soils with and without well-developed cyanobacterial biocrusts in the two study sites. Soil moisture was up to 6.2% and 8.2% higher under cyanobacterial biocrusts than under bare surfaces at El Cautivo (Figure 3a) and Las Amoladeras (Figure 3b), respectively. We also found differences in soil moisture content between soils. Soil moisture was higher under both cyanobacterial biocrusts and bare soils on the sandy loam soils at Las Amoladeras than on the silty loam soils at El Cautivo. This can be partially explained by differences in rainfall. During the study period, rainfall was higher in Las Amoladeras (535 mm year^{-1}) than in El Cautivo (405 mm year^{-1}) which, as observed in Figure 3, affected antecedent soil moisture.
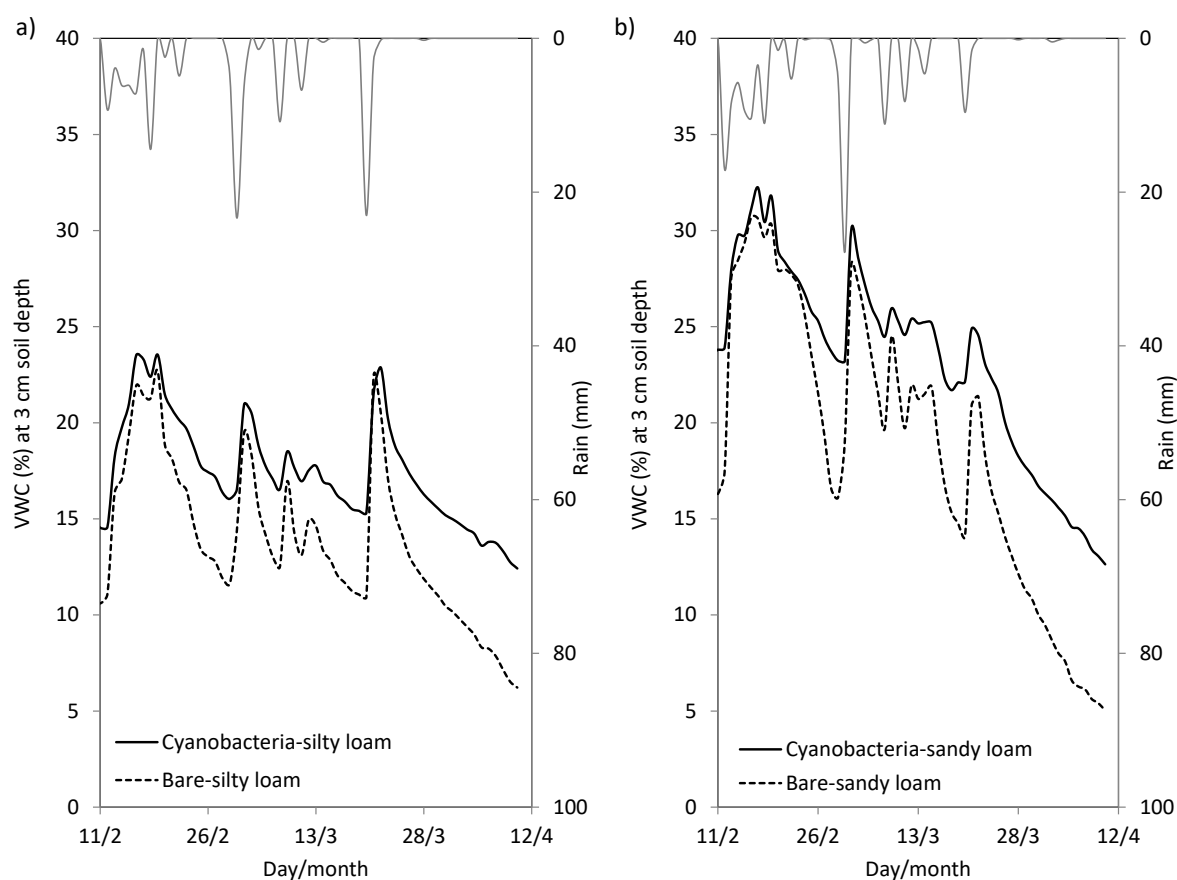
Figure 3. Volumetric water content (VWC, %) during a wet soil period in cyanobacteria-covered and bare soils at both study sites, (**a**) El Cautivo (silty loam soils) and (**b**) Las Amoladeras (sandy loam soils).

Regarding the loss of water by runoff, at plot scale, well-developed cyanobacterial biocrusts from both sites showed similar hydrological responses under simulated extreme rainfall, with runoff coefficients of about 57.9 ± 15.4% and 58.6 ± 11.2% at El Cautivo and Las Amoladeras, respectively (Figure 4). Lower runoff coefficients were found in well-developed cyanobacteria biocrusts compared to incipient ones at El Cautivo (mean values were 64.8 ± 12.7% in IC$_C$ and 57.9 ± 15.4% in C$_C$). We also observed differences in rain to ponding and rain to runoff. Under dry antecedent soil moisture, 0.88 mm of rain was necessary for ponding and 2.60 mm for runoff to start in IC$_C$, whereas in C$_C$ 1.53 mm and 2.70 mm were necessary, respectively.

Similar results were found when runoff was monitored in the field plots under natural rain. Table 2 shows a set of five consecutive rainfall events, differing in amount and intensity, which were recorded during February and March 2010, coinciding with the period shown for soil moisture content in Figure 3. As observed in Table 2, in all events, soils covered by C$_C$ had lower runoff coefficients than

IC$_C$. However, some differences depending on rainfall properties and spatial scales were observed. At plot scale, during high magnitude and high intensity rainfall events, runoff coefficients in IC$_C$ doubled those recorded in C$_C$ (see events on 26 January and 24 February, and 8 March), and differences were even wider in low magnitude and low intensity events (see event on 12 March and on 21 March), where runoff coefficients were up to 4 times higher in IC$_C$ than in C$_C$. At hillslope scale, behavior was similar, and runoff coefficients were lower in C$_C$ than IC$_C$ (Table 2). Runoff rates, in general, decreased as plot size increased, for both C$_C$ and IC$_C$, although for ICc differences were not significant (Figure 5). In fact, in the larger hillslope plots, measured event-scale runoff coefficients were up to seven-fold lower than those measured on the small plots, depending on rainfall properties and previous antecedent soil moisture (Table 2).
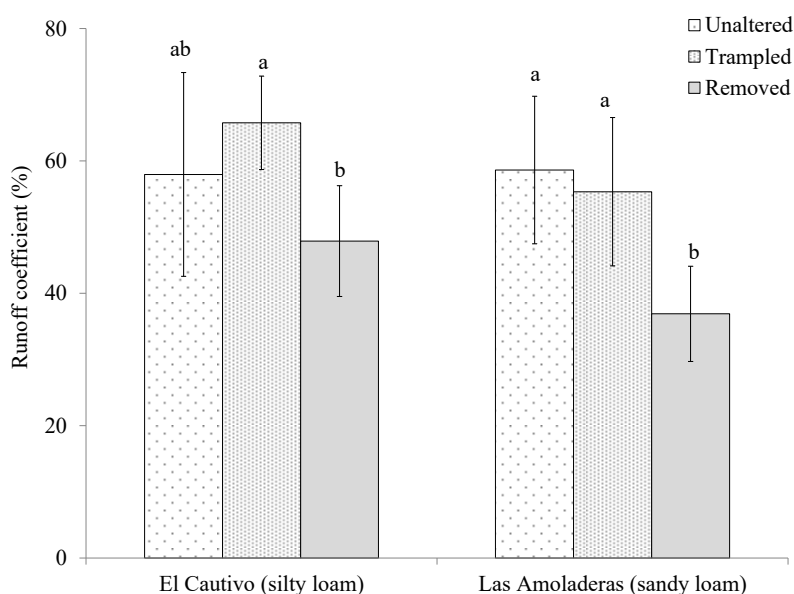

Figure 4. Runoff coefficient (%) in unaltered, trampled and removed well-developed cyanobacterial biocrusts after 1 h of rainfall simulation with a constant intensity of 50 mm h^{-1}, on silty loam (El Cautivo) and sandy loam (Las Amoladeras) soils. Different letters indicate significant differences ($p < 0.05$) among treatments at each site.

Table 2. Characteristics of rainfall events and runoff coefficients (mean ± SD, n = 3) measured in the plots with incipient and well-developed cyanobacterial biocrusts, at the different scales at El Cautivo site.

| | **Rainfall** | | | **Runoff Coefficient (%)** | | | | |
| | | | | **Well-Developed Cyanobacteria (C$_C$)** | | | **Incipient Cyanobacteria (ICc)** | |
Date	**Amount (mm)**	**I$_{mean}$ (mm h^{-1})**	**I$_{max}$ (mm h^{-1})**	**Plot**	**Small Hillslope**	**Large Hillslope**	**Plot**	**Small Hillslope**
SSC (mL)	-		-	47.66	114.18	386.55	12.01	56.89
26 January-10	46	7.1	19.4	18.0 ± 1.8	18.4 ± 3.6	16.0 ± 3.3	35.6 ± 6.3	35.4 ± 10.4
24 Febuary-10	58	4.5	12.2	7.9 ± 0.9	5.9 ± 0.8	3.7 ± 1.3	12.1 ± 3.8	13.6 ± 3.0
8 March-10	37	5.6	23.5	22.1 ± 5.8	5.1 ± 3.8	2.7 ± 1.6	34.9 ± 4.5	17.9 ± 3.6
12 March-10	19	3.4	10.4	2.7 ± 3.5	3.0 ± 4.4	2.4 ± 0.9	11.9 ± 6.8	11.4 ± 2.4
21 March-10	24	1.7	5.8	1.5 ± 2.3	2.4 ± 2.7	1.3 ± 0.2	4.8 ± 3.2	9.6 ± 3.5

SSC: surface storage capacity.
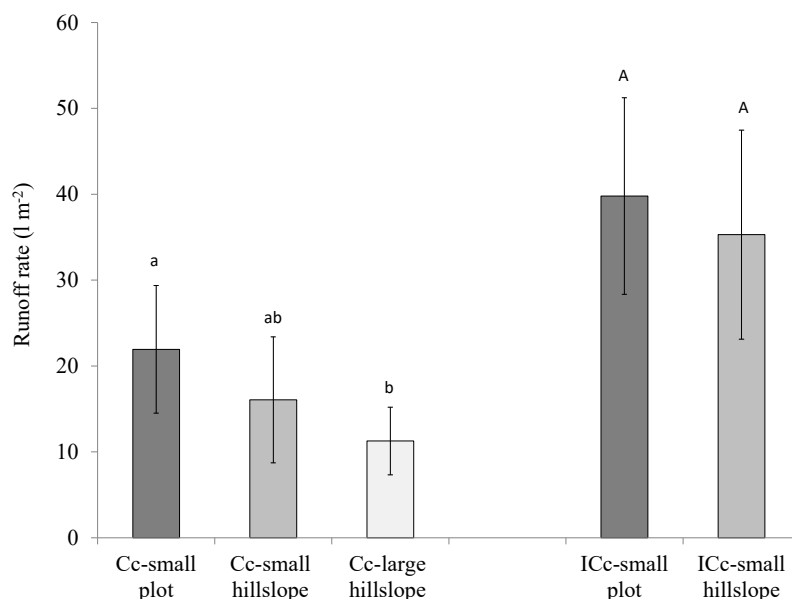
Figure 5. Total runoff rates during the period shown in Table 2 (26 January–21 March 2010) in well-developed cyanobacterial (C_C) and incipient-cyanobacterial (IC_C) biocrusts at El Cautivo, at plot (~1 m²), small-hillslope (~10 m²) and large-hillslope (~20 m²) scales. There were no plots at large-hillslope scale for the IC_C crust. Different letters indicate significant differences ($p < 0.05$) among spatial scales for each crust type.

Regarding the influence of cyanobacterial biocrust on the loss of moisture from soil through evaporation, it was found that the slope of the drying curves during the different drying events analyzed (see Section 2.5) was higher at Las Amoladeras than at El Cautivo, indicating a faster soil drying. At El Cautivo, the soil cover and event had a significant effect on slope, whereas at Las Amoladeras, both had only a marginally significant effect ($p < 0.1$ for both factors, see Table S2 in Supplementary materials). At both sites, the slope was higher in bare soils than in cyanobacterial biocrusts (Figure 6) (mean slope values in bare soils and cyanobacterial biocrusts on silty loam soils were, respectively, -0.008 ± 0.004 and -0.006 ± 0.003 %/day; and -0.80 ± 0.37 and -0.62 ± 0.15 %/day on sandy loam soils). Figure 7 shows the rate of soil water loss during a soil drying period (from 21 March to 12 April). Bare soils lost water faster than cyanobacterial biocrusts, and the difference between both was higher in silty loam than sandy in loam soils (Figure 7). Moreover, water loss from both cyanobacterial biocrusts and bare soils varied depending on soil texture. During the first four days following rainfall, soil water loss was similar in cyanobacterial biocrusts from both textured soils. However, from the fourth day on, water loss was faster in cyanobacterial biocrusts in the sandy loam than in the silty loam soils. On the contrary, bare silty loam soils lost water faster than sandy loam soils during the first 11 days after rainfall, but after that, water losses were similar in both soil textures. After 22 days of soil drying, soils covered by cyanobacterial biocrusts and bare soils had lost 45% and 75%, respectively, of their original water content in silty loam soils, and 54% and 78% of their original water content on sandy loam soils.
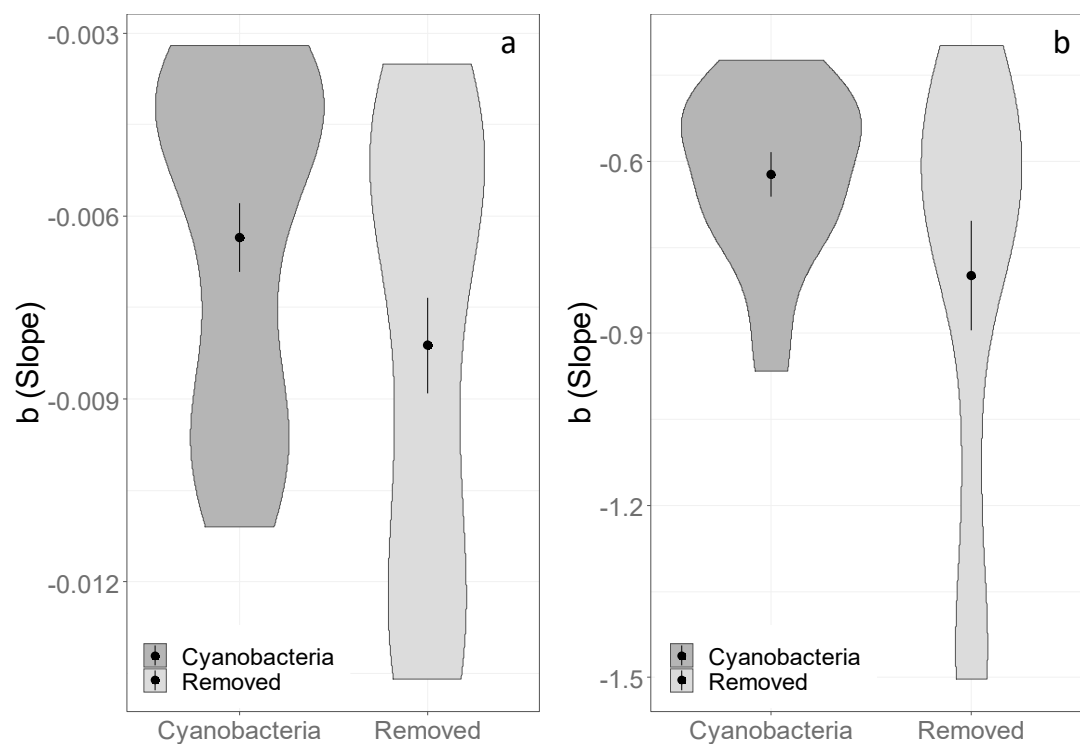
Figure 6. Violin plots showing the distribution of the slope of the drying curves fitted to a linear regression for different soil drying events at (**a**) El Cautivo and (**b**) Las Amoladeras.
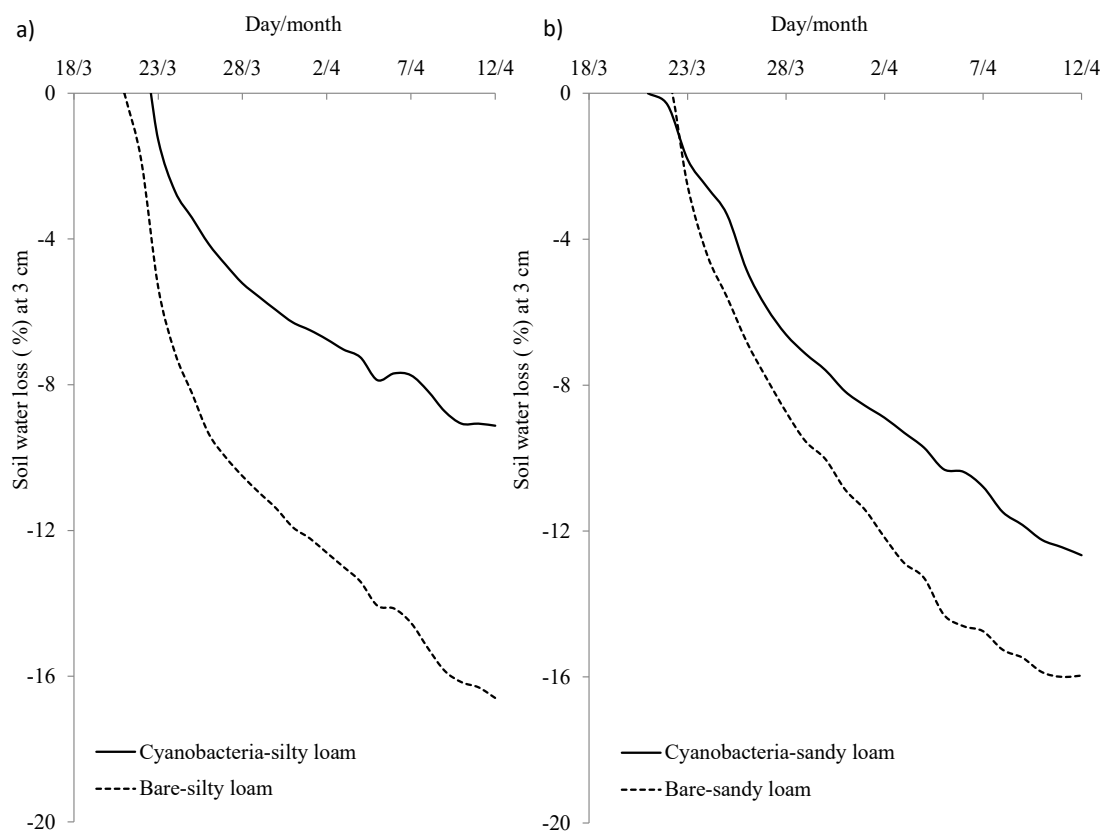

Figure 7. Soil water loss (%) during the drying soil period from 21 March to 12 April 2010 in soils covered by cyanobacterial biocrusts and bare soils (where the biocrust was removed) at both study sites, (**a**) El Cautivo (silty loam soils) and (**b**) Las Amoladeras (sandy loam soils).

3.2. Effects of Cyanobacterial Biocrust Disturbance on Soil Surface Hydrology

Disturbance of cyanobacterial biocrusts altered their influence on hydrological processes. Moreover, this effect varied depending on soil properties. Under the high intense simulated rainfall, we found that runoff was higher on the trampled cyanobacterial biocrusts than on the unaltered ones on silty loam soils. However, almost no difference was found on sandy loam soils (Figure 4). Removal of the crust caused an initial decrease in runoff in both areas. However, after the first few minutes, runoff increased in the scraped soils over time due to soil sealing after raindrop impact and the formation of a structural crust. At the end of the rainfall event, differences in runoff yield between the unaltered cyanobacterial biocrusts and the scraped soils were attenuated (for example, steady state infiltration rates were 16.9 and 21.6 mm h^{-1} in cyanobacterial biocrusts and scraped or bare soils, respectively, at El Cautivo). It is worth noting that particle detachment was significantly increased after biocrust removal. In silty loam soils, sediment yield from the trampled biocrust was three-fold higher than from the undisturbed cyanobacterial biocrust and four-fold higher from soil where biocrust had been removed. In sandy loam soils, both biocrust trampling and removal caused 3.5-fold higher sediment yield than the undisturbed cyanobacterial biocrust (Figure 8).
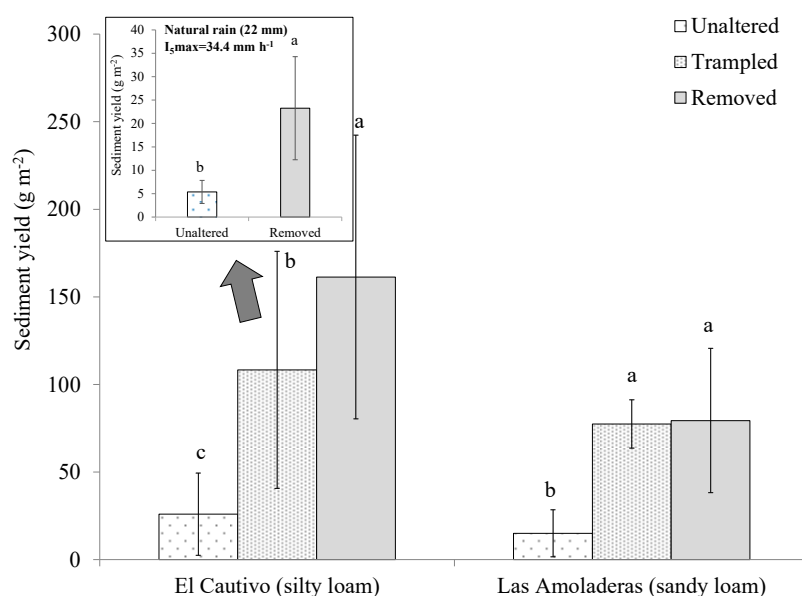

Figure 8. Sediment yield (g m^{-2}) in unaltered, trampled and removed well-developed cyanobacterial biocrusts after 1 h of rainfall simulation with a constant intensity of 50 mmh^{-1}, on silty loam (El Cautivo) and sandy loam (Las Amoladeras) soils. Sediment yield in unaltered and removed cyanobacterial biocrusts during an intense natural rain at El Cautivo is shown in the upper left figure. Different letters indicate significant differences ($p < 0.05$) among treatments at each site.

Removal of cyanobacterial biocrusts also decreased soil moisture content and increased soil water losses. Table 3 shows average soil moisture content and soil water loss during drying in soils covered by cyanobacteria and bare soils where the cyanobacterial biocrust had been removed, following rainfall (20 mm) immediately after biocrust removal. Average soil moisture content during the drying period was higher under cyanobacterial biocrusts than in the bare soils (resulting from cyanobacterial biocrust removal, see Section 2.3) in both silty loam (El Cautivo) and sandy loam soils (Las Amoladeras). After two months of soil drying following rainfall, the percentage of water lost at 3 cm compared to the original water content was higher in soils where biocrusts had been removed than in the unaltered cyanobacterial biocrusts in both types of soil textures.

Table 3. Average volumetric water content (VWC, %) and soil water loss ($VWC_{max} - VWC_{min}/VWC_{max}$, %) at 3 and 10 cm in soils with well-developed cyanobacterial biocrusts and soils after crust removal during a drying period (from 28 September to 28 November) following a rainfall (20 mm) occurred immediately after the biocrust was scraped off.

Soil Surface Type	El Cautivo (Silty Loam Soils)		Las Amoladeras (Sandy Loam Soils)	
	VWC (%)	Soil Water Loss (%)	VWC (%)	Soil Water Loss (%)
Cyanobacteria (3 cm)	7.9	83	11.9	59
Removed crust (3 cm)	5.1	94	8.2	83
Cyanobacteria (10 cm)	16.5	43	19.6	50
Removed crust (10 cm)	14.6	50	13.9	69

The monitoring of the natural recovery of well-developed cyanobacterial biocrusts showed that the first year after removal, total biocrust cover was 26.18 ± 4.80%, with a maximum of 36.7% per plot. It decreased during the second year (12.57 ± 4.80%), and the difference between years was significant (F = 32.54; *p* = 0.0047), showing that the recovery rate was not constant, nor did it increase over time, but on the contrary, regressed considerably. There were differences in rainfall properties between the two years monitored: both the mean number of rainy days per month and the total rainfall volume per month were much higher in the second year than in the first (6.7 rainy days vs. 4.1 rainy days, Kruskal–Wallis H (here after K–W H)(1.96) = 8.54, *p* = 0.0035, and 27 mm vs. 15 mm, K–W H (1.96) = 5.67, *p* = 0.0172). The monthly absolute maximums of rainfall intensity, monthly mean of daily maximums of rainfall intensity and monthly mean of rainfall intensity were also much higher in the second year (K–W H (1.96) = 10.64, *p* = 0.0011; K–W H (1.96) = 6.90, *p* = 0.0086, and K–W H (1.96) = 9.68, *p* = 0.0019, respectively). The monthly average of rainfall intensity was 13.6 mm h^{-1} in the second year and 3.1 mm h^{-1} in the first year. Lichens colonization was also observed. In total 13 lichen species were counted in the plots. Three of the lichen species recorded during the first year disappeared during the second year, and four new ones appeared during the second year, although only one (*Collema* sp.) reached any significant frequency. The highest frequencies corresponded to the macroscopically undifferentiated cyanobacterial biocrusts, which were close to the maximum during the first year (36, the same as the number of grid cells), and remained during the second. Although there were small differences in the number of colonizing lichen species, species identity, and even in frequency between the first and the second year, biodiversity according to the Shannon–Weaver index significantly increased from 2.79 ± 0.082 to 2.87 ± 0.082 (F = 2403.85; *p* < 0.00001).

4. Discussion

Cyanobacterial biocrusts are initial precursors of biocrust succession and many times the dominant community within biocrust, constituting a key biotic component in many drylands. On these ecosystems, where water is a scarce, pulsed and seasonal resource [78], they play an important role in several soil surface properties that regulate the soil water balance. By controlling water availability, they ultimately drive the activity of organisms, and thus the rate of ecosystem processes depending on them, such as biogeochemical cycles [79]. For this reason, understanding how cyanobacterial biocrusts affect soil water balance is key to understand vital dryland ecosystem processes. We found that plots covered with well-developed cyanobacterial biocrusts showed increased infiltration and decreased runoff respect to bare soils. This result combined with the reduced soil water loss from the upper layers and increased water gains from NRWIs, contributed to maintaining a higher soil water availability, which is the most limiting factor in drylands. Our results also confirm that the role that cyanobacterial biocrusts play in hydrological processes is conditioned by their cover, biomass, and roughness, as well as their concomitant effects on underlying soil physicochemical properties. All these properties, and their interactions with site characteristics, rainfall properties and spatial scale, are affected by disturbance and climate change [77,80]. Thus, common disturbances, such as removal or trampling

by human activities, and expected changes in temperature and precipitation, may alter the capacity of cyanobacterial biocrusts to provide water regulation services with an intensity that will strongly depend on site characteristics.

4.1. Role of Cyanobacterial Biocrust in Soil Surface Hydrology

Many dryland soils are characterized by low organic matter content and poor soil structure [81]. Fine particle soils with these properties often lead to the formation of a physical soil crust with a low-porosity layer at the soil surface. This crust decreases hydraulic conductivity, limits infiltration, and favors the generation of runoff [82–84]. Cyanobacterial colonization on these soils usually enhances microtopography [29,41], improves soil aggregation and stability [22] and increases porosity [85,86], thereby enhancing infiltration. Thus, at the El Cautivo site, increased roughness in the more developed cyanobacterial biocrusts (Cc), in relation to the incipient ones (ICc), (Table 1) surely contributes to facilitate water percolation into the soil [29,41,85]. At this site, ks (Table 1) and the amount of rainfall to runoff start increased on the well-developed cyanobacterial biocrust, under both the simulated extreme and natural rainfall (see Section 3.1). Cyanobacterial colonization on these soils also enhances EPS content (Table 1) and, as a result, several surface properties related to their hydrological behavior improve. EPS content in C_C and C_A was respectively 2 and 4.4 times higher than in IC_C (Table 1), agreeing with previous results which have found 1.5 to 3 times higher EPS content in soil samples with a high than a low cyanobacterial cover [87]. EPS can increase hydraulic conductivity on silty soils by improving soil aggregation and macroporosity, thus creating pathways for water infiltration [88]. In this sense, Miralles-Mellado et al. [85] found that pore occurrence in soils covered by cyanobacteria was related to EPS and the ability of filaments to adhere to one another and bind soil particles, and hence affect the soil's spatial organization. Besides, the capacity of cyanobacteria to secrete EPS compounds strongly increases organic carbon content [22,89] and water retention capacity of soils [90]. It has been shown that water holding capacity at field capacity can be 1.2 times higher (on silty loam soils, [31]) or from 2 to 4 times higher (on sandy soils, [85]) in soils with high than with low cyanobacterial cover. Thus, at El Cautivo site, water holding capacity at −33kPa was 23.6% and 28.7% (gravimetric) in IC_C and C_C, respectively [37]. The influence of EPS secretion on porosity is also reflected in the results reported by [86], who found at El Cautivo, 3.5% of the total area under IC_C occupied by pores, while under more developed biocrusts the pores occupied from 11.6 ± 1.5 to 23.7 ± 4%. The same study also found that, in addition to the pore area, cyanobacterial developmental stage modified pore sizes and geometry. Pore shapes changed from tortuous to straight as cyanobacteria developed [86]. The predominance of vesicle pores [86] under IC_C undoubtedly plays an important role in reducing infiltration (Table 2) compared to C_C, which has higher meso- and macro-porosity.

Sandy soils are less susceptible to develop physical crusts and often have higher infiltration rates than fine-textured soils [91]. In these soils, cyanobacteria colonization may increase runoff compared to bare soils due to pore clogging by swollen EPS [92] and the consequent decrease in effective porosity [85]. In these cases, cyanobacterial biocrusts have been described to rapidly generate runoff and provide additional water to plants downslope [93]. In our study sites, well-developed cyanobacterial biocrusts showed similar runoff coefficients in silty loam and sandy loam soils during simulated rainfall (Figure 4). Lower underlying silty soil infiltration capacity at El Cautivo was probably compensated by the rougher crust at this site than at Las Amoladeras.

In addition to the observed effect on infiltration-runoff, we found that NRWI deposition was higher on cyanobacterial biocrust than on bare soil (Figure 2). Similar results have been found by other authors [94,95], who have attributed this higher dewfall deposition/water vapour adsorption in cyanobacterial biocrusts to their higher EPS content [96,97]. Higher surface roughness of cyanobacterial crusts when compared to bare soils is probably another important factor affecting this process, as it increases the tortuosity and area for water absorption. Due to greater variability in EPS, cover and roughness among C_C samples (Table 1), NRWI amount showed higher variability in C_C than in bare soils (Figure 2). Water gains by NRWIs are suggested as a crucial source of water for growth and

development of biocrusts in extremely harsh environments [98]. Cyanobacteria are able to survive long droughts, when their metabolic activity ceases, and again become active with very little water amount of around 0.1 mm, such as that available during the early hours of the day after dew events [99].

On the whole, higher NRWIs (Figure 2) and infiltration (Table 2) in cyanobacterial biocrusts along with a higher available water storage capacity (Table 1) and lower water losses (Figures 6 and 7) explain the higher soil moisture in these soils respect bare soils (Figure 3). Underlying soil properties also play an important role. For example, C_A lost water faster (Figures 6 and 7) due to the lower water retention capacity of the underneath sandy soil (Table 1). It should be noted that the higher moisture content in soils covered by cyanobacterial biocrusts was only observable during periods of high soil water content. During dry soil periods, water losses have been reported to be similar in both cyanobacteria-covered and bare soils. This is attributed to the decreasing soil pore blocking effect as the crust dries, resulting in similar moisture content whether soil has cyanobacterial biocrusts or not [48].

While the hydrological responses of cyanobacterial biocrusts at plot scale have been more thoroughly investigated, scarce studies have been conducted at the larger hillslope scale. Our results show that hillslope and plot-scale patterns were similar, with C_C showing lower runoff coefficients than IC_C. However, we found some differences in runoff generation among the different spatial scales (Table 2, Figure 5) due to the well-known scale effect [24,100]. Cyanobacterial cover and biomass increase surface roughness and total volume of micro-depressions [29,41], which slow down overland flow, acting as temporary runoff sinks and reducing flow connectivity [101]. Moreover, small pools of water in microdepressions lead to higher hydraulic head, increasing infiltration [29,102]. This effect increases from small plot to hillslope scale [29] and was reflected by the increase in SSC from the plot to the small and large hillslope scale, resulting in a significant decrease in runoff yield in well-developed biocrusts at coarser scales (Figure 5). In the smoother IC_C, SSC was much lower (see Table 2) and differences in SSC between plot and hillslope were less accentuated, and as a result, runoff did not significantly differ between plot and hillslope scale. These results are important because of the fact that, compared to vegetated areas, cyanobacterial biocrusts act as runoff sources, providing runoff and increasing water availability to vegetation, thereby having an important effect on the survival and productivity of vegetation. However, the ability of vegetation to reinfiltrate runoff from cyanobacteria-crusted areas is limited and during some very intense events it can be overwhelmed [38,103]. During these events, concentrated water flows with more erosive power may be generated downstream [24]. Therefore, to properly determine the role of dryland ecosystems on the provision of water and erosion regulating services to the society, the role of cyanobacterial biocrusts in hydrological processes and how they interact with other surface components as well as the spatial distribution of cyanobacterial biocrusts and other types of biocrust, need to be quantified [104].

4.2. Effects of Disturbance of Cyanobacterial Biocrusts on Soil Hydrology

Despite their importance, global drylands are being degraded through a complex combination of human alterations (i.e., overgrazing, deforestation), which have demonstrated to be dramatic for biocrusts [105,106]. In a similar way, as climate change, the physical disturbance of biocrusts reduces biocrust coverage and shift biocrust composition from well-developed biocrusts to early light cyanobacteria dominated biocrusts [80]. This is expected to alter hydrological processes. For example, trampling the biocrusts leads to less surface roughness and increased soil compaction, especially on fine-textured soils, thus increasing runoff (Figure 4). Removal of cyanobacterial biocrusts, on the contrary, initially increases infiltration (Figure 4). However, even just one heavy rainfall event can cause new raindrop-induced surface seals to form, leading to a physical soil crust making runoff higher than on unaltered cyanobacterial biocrusts [32]. As a result of all these changes arising from cyanobacterial biocrust disturbance, decreased soil moisture content is expected and the consequent decrease in water availability for soil microbial communities living in the upper soil horizons in space among plants (Table 3). As a result, changes in C and N fixation, decomposition of organic compounds,

and mineralization of N are foreseen, and, in general, alterations in other processes triggered by soil microbe activity, that in turn, will affect the composition and structure of plant communities [107].

In addition to decreasing infiltration, cyanobacterial biocrust disturbance dramatically increased sediment yield (Figure 8) as other authors found in cyanobacteria and other biocrust types [32,43,108]. These consequences were more noticeable in silty loam than sandy loam soils, not only because fine-textured soils are more susceptible to water erosion, but also because of the higher runoff rates observed in these soils after biocrust removal (Figure 4). Increased water erosion after cyanobacterial biocrusts removal has also been demonstrated to significantly influence organic carbon losses by increasing runoff and water erosion [53,109–111]. Cantón et al. [54] found that under simulated extreme rainfall, plot-scale organic carbon losses increased from 3.4 to 5.6 g m^{-2} after removal of incipient cyanobacterial biocrusts and tripled after removal of well-developed cyanobacterial biocrusts (from 1.2 to 4 g m^{-2}). Consequently, cyanobacterial biocrust loss and their replacement by a physical soil crust will decrease carbon inputs by photosynthesis, and increase organic carbon losses by runoff and erosion. This may reduce the ability of soils to trap nutrient-enriched dust [112], alter the balanced transfer of organic carbon and nutrients to vegetated patches and lead to a reduction in cover and size of vegetation patches [113]. Runoff water, sediments and nutrients will flow through preferential paths increasing hillslope connectivity, and thus the total amount of system water and nutrient lost, reducing ecosystem functioning and productivity [114].

After a disturbance, with formation of incipient cyanobacterial biocrust, photoautotrophic organisms increase, organic matter gradually accumulates in soil, accelerating the growth of heterotrophic microbes, which transform organic matter into inorganic compounds, providing nutrients for photoautotrophic organisms, and thus promoting a positive feedback mechanism [115]. However, the time required for the recovery of the developed cyanobacterial biocrust seems to be quite variable [3] depending on climate and soil stability conditions. Our results showed that one year after the biocrust removal, the cyanobacterial biocrust cover had increased to 37%. However, cyanobacterial biocrust cover did not follow an increasing trend over time, and on the contrary, during the second year of recovery, the cyanobacterial biocrust cover decreased. The significantly wide differences in amount and features of rainfall during the two studied years were identified as the main causes affecting biocrust growth. A higher biocrust growth would have been expected because of the larger amount of rainfall during the second year. However, the stronger rainfall intensities may have dismantled part of the cyanobacterial biocrust in development. Similarly, [111] reported that raindrop impact during intense rainfall could damage unconsolidated biocrusts and cause cyanobacterial cover to decline. Given the uncertainty in the natural restoration of the cyanobacterial biocrust after disturbance and the important functions they play maintaining several regulating services in dryland ecosystems, the risk of adverse effects that may cause anthropogenic forces should be previously set out.

5. Conclusions

Differences in water regulation capacity were found between dryland soils covered by cyanobacterial biocrust and bare ones. Water availability was higher in cyanobacterial biocrusts compared to bare soils as a result of their influence enhancing infiltration, soil moisture content, and NRWIs, and reducing evaporation. These effects were modulated by the characteristics of the site, such as soil texture, rainfall properties or spatial scale. The developmental stage of the cyanobacterial biocrust was also significant to understand its hydrological behavior. Runoff decreased as biocrust development increased, being this effect evident at both plot and hillslope scales, and resulting in higher moisture retention in well-developed compared to incipient cyanobacterial biocrusts.

Disturbance of the cyanobacterial biocrusts through anthropogenic drivers affects their roles in hydrological processes, decreasing water gains during most dew and rainfall events and enhancing soil water losses, which, in the end, resulted in a diminution of water availability at the top soil. In addition, cyanobacterial biocrust disturbance, especially when the biocrust is removed, strongly

increases erosion, which has important consequences for carbon loss and nutrient redistribution within the ecosystem.

Given the multiple and important roles that cyanobacterial biocrusts play controlling different processes that support the capacity of dryland ecosystems to provide key services, such as water regulation or erosion control, together with their vulnerability to anthropic disturbances and later uncertain natural restoration, efforts to conserve and restore them, when necessary, deserve to be considered. For that, it is essential to translate their relevance for maintaining ecosystem services to local communities and the different actors involved in the management of these ecosystems.

Supplementary Materials: The following are available online at http://www.mdpi.com/2073-4441/12/3/720/s1, Table S1: Summary of General Linear Mixed Models (LMMs) for Non-Rainfall Water Inputs (NRWI) during dry, wet soil periods and for the total study period, as a function of cover type (well-developed cyanobacterial crusts and bare soil), and NRWI event; Table S2: Summary of General Linear Mixed Models (LMMs) for soil moisture decrease rate, as a function of cover type (well-developed cyanobacterial crusts and bare soil), and drying event at the two study sites (El Cautivo and Las Amoladeras).

Conflicts of Interest: The authors declare no conflict of interest.

References

1. Rodriguez-Caballero, E.; Belnap, J.; Büdel, B.; Crutzen, P.J.; Andreae, M.O.; Pöschl, U.; Weber, B. Dryland photoautotrophic soil surface communities endangered by global change. *Nat. Geosci.* **2018**, *11*, 185–189. [CrossRef]

2. Weber, B.; Büdel, B.; Belnap, J. *Biological Soil Crusts: An Organizing Principle in Drylands*, 2nd ed.; Springer: Berlin/Heidelberg, Germany, 2016.

3. Belnap, J.; Lange, O.L. *Biological Soil Crusts: Structure, Function and Management*, 1st ed.; Springer: Berlin/Heidelberg, Germany, 2003.

4. Belnap, J.; Rosentreter, R.; Leonard, S.; Kaltenecker, J.H.; Williams, J.; Eldridge, D. *Biological Soil Crusts: Ecology and Management, Department Series*; US Department of the Interior, Bureau of Land Management, and National Science and Technology Center: Denver, CO, USA, 2001; p. 210.

5. Kumar, D.; Adhikary, S.P. Diversity, molecular phylogeny, and metabolic activity of cyanobacteria in biological soil crusts from Santiniketan (India). *J. Appl. Phycol.* **2014**, *27*, 331. [CrossRef]

6. Kosten, S.; Huszar, V.L.M.; Bécares, E.; Costa, L.S.; van Donk, E.; Hansson, L.A.; Jeppesen, E.; Kruk, C.; Lacerot, G.; Mazzeo, N.; et al. Warmer climates boost cyanobacterial dominance in shallow lakes. *Glob. Chang. Biol.* **2012**, *18*, 118–126. [CrossRef]

7. Pointing, S.B.; Büdel, B.; Convey, P.; Gilman, L.N.; Körner, C.; Leuzinger, S.; Vincent, W.F. Biogeography of photoautotrophs in the high polar biome. *Front. Plant Sci.* **2015**, *6*, 692. [CrossRef] [PubMed]

8. Rajeev, L.; da Rocha, U.N.; Klitgord, N.; Luning, E.G.; Fortney, J.; Axen, S.D.; Shih, P.M.; Bouskill, N.J.; Bowen, B.P.; Kerfeld, C.A.; et al. Dynamic cyanobacterial response to hydration and dehydration in a desert biological soil crust. *ISME J.* **2013**, *7*, 2178–2191. [CrossRef] [PubMed]

9. Oren, A. Salts and Brines. In *Ecology of Cyanobacteria II: Their Diversity in Space and Time*; Whitton, B.A., Ed.; Springer: Berlin/Heidelberg, Germany, 2012; pp. 401–420.

10. Castenholz, R.W.; Garcia-Pichel, F. Cyanobacterial Responses to UV Radiation. In *Ecology of Cyanobacteria II: Their Diversity in Space and Time*; Whitton, B.A., Ed.; Springer: Berlin/Heidelberg, Germany, 2012; pp. 481–499.

11. Barger, N.N.; Weber, B.; Garcia-Pichel, F.; Zaady, E.; Belnap, J. Patterns and controls on nitrogen cycling of biological soil crusts. In *Biological Soil Crusts: An Organizing Principle in Drylands*, 2nd ed.; Weber, B., Büdel, B., Belnap, J., Eds.; Springer: Berlin/Heidelberg, Germany, 2016; pp. 257–285.

12. Williams, W.; Büdel, B.; Williams, S. Wet season cyanobacterial N enrichment highly correlated with species richness and Nostoc in the northern Australian savannah. *Biogeosciences* **2018**, *15*, 2149–2159. [CrossRef]

13. Pointing, S.B.; Belnap, J. Microbial colonization and controls in dryland systems. *Nat. Rev. Microbiol.* **2012**, *10*, 551–562. [CrossRef]

14. Zhang, B.; Zhang, Y.; Downing, A.; Niuc, Y. Distribution and composition of cyanobacteria and microalgae associated with biological soil crusts in the Gurbantunggut Desert, China. *Arid Land. Res. Manag.* **2011**, *25*, 275–293. [CrossRef]

15. DeFalco, L.A.; Detling, J.K.; Tracy, C.R.; Warren, S.D. Physiological variation among native and exotic winter annual plants associated with microbiotic crust in the Mojave Desert. *Plant Soil* **2001**, *234*, 1–14. [CrossRef]

16. Boeken, B.; Ariza, C.; Gutterman, Y.; Zaady, E. Environmental factors affecting dispersal, germination and distribution of Stipa capensis in Negev Desert, Israel. *Ecol. Res.* **2004**, *19*, 533–540. [CrossRef]

17. Miralles-Mellado, I.; Ladrón de Guevara, M.; Chamizo, S.; Rodríguez-Caballero, E.; Ortega, R.; van Wesemael, B.; Cantón, Y. Soil CO_2 exchange controlled by the interaction of biocrust successional stage and environmental variables in two semiarid ecosystems. *Soil Biol. Biochem.* **2018**, *124*, 11–23. [CrossRef]

18. Powell, J.T.; Chatziefthimiou, A.D.; Banack, S.A.; Cox, P.A.; Metcalf, J.S. Desert crust microorganisms, their environment, and human health. *J. Arid Environ.* **2015**, *112*, 127–133. [CrossRef]

19. Elbert, W.; Weber, B.; Burrows, S.; Steinkamp, J.; Büdel, B.; Andreae, M.O.; Pöschl, U. Contribution of cryptogamic covers to the global cycles of carbon and nitrogen. *Nat. Geosci.* **2012**, *5*, 459–462. [CrossRef]

20. Robertson, G.P.; Groffman, P.M. Nitrogen transformations. In *Soil Microbiology, Biochemistry and Ecology*; Paul, E.A., Ed.; Springer: Berlin/Heidelberg, Germany, 2007; pp. 341–364.

21. Rossi, F.; Li, H.; Liu, Y.; De Philippis, R. Cyanobacterial inoculation (cyanobacterisation): Perspectives for the development of a standardized multifunctional technology for soil fertilization and desertification reversal. *Earth Sci. Rev.* **2017**, *171*, 28–43. [CrossRef]

22. Chamizo, S.; Mugnai, G.; Rossi, F.; Certini, G.; De Philippis, R. Cyanobacteria inoculation improves soil stability and fertility on different textured soils: Gaining insights for applicability in soil restoration. *Front. Environ. Sci.* **2018**, *6*, 49. [CrossRef]

23. Cantón, Y.; Domingo, F.; Solé-Benet, A.; Puigdefábregas, J. Hydrological and erosion response of a badlands system in semiarid SE Spain. *J. Hydrol.* **2001**, *252*, 65–84. [CrossRef]

24. Cantón, Y.; Solé-Benet, A.; de Vente, J.; Boix-Fayos, C.; Calvo-Cases, A.; Asensio, C.; Puigdefábregas, J. A review of runoff generation and soil erosion across scales in semiarid south-eastern Spain. *J. Arid Environ.* **2011**, *75*, 1254–1261. [CrossRef]

25. Bowker, M.A.; Belnap, J.; Bala-Chaudhary, V.; Johnson, N.C. Revisiting classic water erosion models in drylands: The strong impact of biological soil crusts. *Soil Biol. Biochem.* **2008**, *40*, 2309–2316. [CrossRef]

26. Chamizo, S.; Rodríguez-Caballero, E.; Cantón, Y.; Asensio, C.; Domingo, F. Penetration resistance of biological soil crusts and its dynamics after crust removal: Relationships with runoff and soil detachment. *Catena* **2015**, *126*, 164–172. [CrossRef]

27. Belnap, J.; Walker, B.J.; Munson, S.M.; Gill, R.A. Controls on sediment production in two U.S. deserts. *Aeolian Res.* **2014**, *14*, 15–24. [CrossRef]

28. Zhao, Y.; Qin, N.; Weber, B.; Xu, M. Response of biological soil crusts to raindrop erosivity and underlying influences in the hilly Loess Plateau region, China. *Biodivers. Conserv.* **2014**, *23*, 1669–1686. [CrossRef]

29. Rodríguez-Caballero, E.; Cantón, Y.; Chamizo, S.; Afana, A.; Solé-Benet, A. Effects of biological soil crusts on surface roughness and implications for runoff and erosion. *Geomorphology* **2012**, *145–146*, 81–89. [CrossRef]

30. Felde, V.J.M.N.L.; Peth, S.; Uteau-Puschmann, D.; Drahorad, S.; Felix-Henningsen, P. Soil microstructure as an under-explored feature of biological soil crust hydrological properties: Case study from the NW Negev Desert. *Biodivers. Conserv.* **2014**, *64*, 133–140. [CrossRef]

31. Chamizo, S.; Cantón, Y.; Miralles, I.; Domingo, F. Biological soil crust development affects physicochemical characteristics of soil surface in semiarid ecosystems. *Soil Biol. Biochem.* **2012**, *49*, 96–105. [CrossRef]

32. Chamizo, S.; Cantón, Y.; Lázaro, R.; Solé-Benet, A.; Domingo, F. Crust composition and disturbance drive Infiltration through biological soil crusts in semiarid ecosystems. *Ecosystems* **2012**, *15*, 148–161. [CrossRef]

33. Rodríguez-Caballero, E.; Cantón, Y.; Chamizo, S.; Lázaro, R.; Escudero, A. Soil loss and runoff in semiarid ecosystems: A complex interaction between biological soil crusts, micro-topography, and hydrological drivers. *Ecosystems* **2013**, *16*, 1–18. [CrossRef]

34. Chamizo, S.; Cantón, Y.; Rodríguez-Caballero, E.; Domingo, F.; Escudero, A. Runoff at contrasting scales in a semiarid ecosystem: A complex balance between biological soil crust features and rainfall characteristics. *J. Hydrol.* **2012**, *452–453*, 130–138. [CrossRef]

35. Cantón, Y.; Domingo, F.; Solé-Benet, A.; Puigdefábregas, J. Influence of soil-surface types on the overall runoff of the Tabernas badlands (south-east Spain): Field data and model approaches. *Hydrol. Process.* **2002**, *16*, 2621–2643. [CrossRef]

36. Ludwig, J.A.; Tongway, D.J. Spatial organisation of landscapes and its function in semi-arid woodlands, Australia. *Landscape Ecol.* **1995**, *10*, 51–63. [CrossRef]

37. Puigdefábregas, J. The role of vegetation patterns in structuring runoff and sediment fluxes in drylands. *Earth Surf. Proc. Land* **2005**, *30*, 133–147. [CrossRef]

38. Rodríguez-Caballero, E.; Cantón, Y.; Lázaro, R.; Solé-Benet, A. Cross-scale interactions between surface components and rainfall properties. Non-linearities in the hydrological and erosive behaviour of semiarid catchments. *J. Hydrol.* **2014**, *517*, 815–825. [CrossRef]

39. Malam Issa, O.; Valentin, C.; Rajot, J.L.; Cerdan, O.; Desprats, J.F.; Bouchet, T. Runoff generation fostered by physical and biological crusts in semi-arid sandy soils. *Geoderma* **2011**, *167–168*, 22–29. [CrossRef]

40. Belnap, J.; Wilcox, B.P.; Van Scoyoc, M.V.; Phillips, S.L. Successional stage of biological soil crusts: An accurate indicator of ecohydrological condition. *Ecohydrology* **2012**, *6*, 474–482. [CrossRef]

41. Kidron, G.J.; Monger, H.C.; Vonshak, A.; Conrod, W. Contrasting effects of microbiotic crusts on runoff in desert surfaces. *Geomorphology* **2012**, *139–140*, 484–494. [CrossRef]

42. Chamizo, S.; Cantón, Y.; Rodríguez-Caballero, E.; Domingo, F. Biocrusts positively affect the soil water balance in semiarid ecosystems. *Geomorphology* **2016**, *9*, 1208–1221. [CrossRef]

43. Faist, A.M.; Herrick, J.E.; Belnap, J.; Van Zee, W.; Barger, N.N. Biological soil crust and disturbance controls on surface hydrology in a semi-arid ecosystem. *Ecosphere* **2017**, *8*, e01691. [CrossRef]

44. George, D.B.; Roundy, B.A.; St. Clair, L.L.; Johansen, J.R.; Schaalje, G.B.; Webb, B.L. The effects of microbiotic soil crusts on soil water loss. *Arid Land Res. Manag.* **2003**, *17*, 113–125. [CrossRef]

45. Almog, R.; Yair, A. Negative and positive effects of topsoil biological crusts on water availability along a rainfall gradient in a sandy arid area. *Catena* **2007**, *70*, 437–442.

46. Kidron, G.J.; Tal, S.Y. The effect of biocrusts on evaporation from sand dunes in the Negev Desert. *Geoderma* **2012**, *179–180*, 104–112. [CrossRef]

47. Chamizo, S.; Cantón, Y.; Domingo, F.; Belnap, J. Evaporative losses from soils covered by physical and different types of biological soil crusts. *Hydrol. Process.* **2013**, *27*, 324–332. [CrossRef]

48. Chamizo, S.; Cantón, Y.; Lázaro, R.; Domingo, F. The role of biological soil crusts in soil moisture dynamics in two semiarid ecosystems with contrasting soil textures. *J. Hydrol.* **2013**, *489*, 74–84. [CrossRef]

49. Whitney, K.M.; Vivoni, E.R.; Duniway, M.C.; Bradford, J.B.; Reed, S.C.; Belnap, J. Ecohydrological role of biological soil crusts across a gradient in levels of development. *Geomorphology* **2017**, e1875. [CrossRef]

50. Kuske, C.R.; Yeager, C.M.; Johnson, S.; Ticknor, L.O.; Belnap, J. Response and resilience of soil biocrust bacterial communities to chronic physical disturbance in arid shrublands. *ISME J.* **2012**, *6*, 886–897. [CrossRef] [PubMed]

51. Dojani, S.; Kauff, F.; Weber, B.; Budel, B. Genotypic and phenotypic diversity of cyanobacteria in biological soil crusts of the Succulent Karoo and Nama Karoo of southern Africa. *Microb. Ecol.* **2014**, *67*, 286–301. [CrossRef] [PubMed]

52. Steven, B.; Belnap, J.; Kuske, C.R. Chronic physical disturbance substantially alters the response of biological soil crusts to a wetting pulse, as characterized by metatranscriptomic sequencing. *Front. Microbiol.* **2018**, *9*, 2382. [CrossRef] [PubMed]

53. Barger, N.N.; Herrick, J.E.; Van Zee, J.; Belnap, J. Impacts of biological soil crust disturbance and composition on C and N loss from water erosion. *Biogeochemistry* **2006**, *77*, 247–263. [CrossRef]

54. Cantón, Y.; Román, J.R.; Chamizo, S.; Rodríguez-Caballero, E.; Moro, M.J. Dynamics of organic carbon losses by water erosion after biocrust removal. *J. Hydrol. Hydromech.* **2014**, *62*, 253–257. [CrossRef]

55. Cantón, Y.; Solé-Benet, A.; Lázaro, R. Soil–geomorphology relations in gypsiferous materials of the Tabernas Desert (Almería, SE Spain). *Geoderma* **2003**, *115*, 193–222. [CrossRef]

56. Cantón, Y.; Del Barrio, G.; Solé-Benet, A.; Lázaro, R. Topographic controls on the spatial distribution of ground cover in a semiarid badlands area. *Catena* **2004**, *55*, 341–365. [CrossRef]

57. Rey, A.; Pegoraro, E.; Oyonarte, C.; Were, A.; Escribano, P.; Raimundo, J. Impact of land degradation on soil respiration in a steppe (Stipa tenacissima L.) semi-arid ecosystem in the SE of Spain. *Soil Biol. Biochem.* **2011**, *43*, 393–403. [CrossRef]

58. Lázaro, R.; Cantón, Y.; Solé-Benet, A.; Bevan, J.; Alexander, R.; Sancho, L.G.; Puigdefábregas, J. The influence of competition between lichen colonization and erosion on the evolution of soil surfaces in the Tabernas badlands (SE Spain) and its landscape effects. *Geomorphology* **2008**, *102*, 252–266. [CrossRef]

59. Bevan, J. Dynamics of Lichen Dominated Biological Soil Crusts in the El Cautivo Badlands Southeast Spain. Ph.D. Thesis, University of Chester, Chester, UK, 2009.

60. Maier, S.; Schmidt, T.S.B.; Zheng, L.; Peer, T.; Wagner, V.; Grube, M. Analyses of dryland biological soil crusts highlight lichens as an important regulator of microbial communities. *Biodivers. Conserv.* **2014**, *23*, 1735–1755. [CrossRef]

61. Büdel, B.; Colesie, C.; Green, T.A.; Grube, M.; Suau, R.L.; Loewen-Schneider, K.; Maier, S.; Peer, T.; Pintado, A.; Raggio, J.; et al. Improved appreciation of the functioning and importance of biological soil crusts in Europe: The Soil Crust International Project (SCIN). *Biodivers. Conserv.* **2014**, *23*, 1639–1658. [CrossRef] [PubMed]

62. Roncero-Ramos, B.; Muñoz-Martín, M.A.; Chamizo, S.; Fernández-Valvuena, L.; Mendoza, D.; Perona, E.; Cantón, Y.; Mateo, P. Polyphasic evaluation of key cyanobacteria in biocrusts from the most arid region in Europe. *Peer J.* **2019**, *7*, e6169. [CrossRef] [PubMed]

63. Muñoz-Martín, M.A.; Becerra-Absalón, I.; Perona, E.; Fernández-Valvuena, L.; Garcia-Pichel, F.; Mateo, P. Cyanobacterial biocrust diversity in Mediterranean ecosystems along a latitudinal and climatic gradient. *New Phytol.* **2019**, *22*, 123–141. [CrossRef] [PubMed]

64. Clark, R.N.; Roush, T.L. Reflectance spectroscopy. Quantitative analysis techniques for remote sensing applications. *J. Geophys. Res.* **1984**, *89*, 6329–6340. [CrossRef]

65. Rossi, F.; Mugnai, G.; De Philippis, R. Complex role of the polymeric matrix in biological soil crusts. *Plant Soil* **2018**, *429*, 19–34. [CrossRef]

66. Dubois, M.; Gilles, K.A.; Hamilton, J.K.; Rebers, P.A.; Smith, F. Colorimetric method for determination of sugars and related substances. *Anal. Chem.* **1956**, *28*, 350–356. [CrossRef]

67. Castle, S.C.; Morrison, C.D.; Barger, N.N. Extraction of chlorophyll a from biological soil crusts: A comparison of solvents for spectrophotometric determination. *Soil Biol. Biochem.* **2011**, *43*, 853–856. [CrossRef]

68. Ritchie, R. Consistent sets of spectrophotometric chlorophyll equations for acetone, methanol and ethanol solvents. *Photosynth. Res.* **2006**, *89*, 27–41. [CrossRef]

69. Mingorance, M.D.; Barahona, E.; Fernández-Gálvez, J. Guidelines for improving organic carbon recovery by the wet oxidation method. *Chemosphere* **2007**, *68*, 409–413. [CrossRef] [PubMed]

70. Bremner, J.M. Nitrogen-total. In *Methods of Soil Analysis. Part 3, Chemical Methods*; Sparks, D.L., Ed.; SSSA-ASA: Madison, WI, USA, 1996; pp. 1085–1121.

71. Imeson, A.C.; Vis, M. Assessing soil aggregate stability by ultrasonic dispersion and water-drop impact. *Geoderma* **1984**, *34*, 185–200. [CrossRef]

72. Zhang, R. Determination of soil sorptivity and hydraulic conductivity from the disk infiltrometer. *Soil Sci. Soc. Am. J.* **1997**, *61*, 1024–1030. [CrossRef]

73. Calvo-Cases, A.; Gisbert, B.; Palau, E.; Romero, M. Un Simulador de Lluvia de fácil Construcción. In *MÉtodos y Técnicas para la Medición en el Campo de Procesos Geomorfológicos*; Sala, M., Gallart, F., Eds.; Sociedad Española de Geomorfología: Zaragoza, Spain, 1988; Volume 1, pp. 6–15.

74. Uclés, O.; Villagarcía, L.; Cantón, Y.; Domingo, F. Microlysimeter station for long term non-rainfall water input and evaporation studies. *Agric. Forest Meteorol.* **2013**, *182–183*, 13–20. [CrossRef]

75. Lafuente, A.; Berdugo, M.; Ladrón de Guevara, M.; Gozalo, B.; Maestre, F.T. Simulated climate change affects how biocrusts modulate water gains and desiccation dynamics after rainfall events. *Ecohydrology* **2018**, *11*, e1935. [CrossRef] [PubMed]

76. Román, J.R.; Rodríguez-Caballero, E.; Rodríguez-Lozano, B.; Roncero-Ramos, B.; Chamizo, S.; Águila-Carricondo, P.; Cantón, Y. Spectral Response Analysis: An Indirect and Non-Destructive Methodology for the Chlorophyll Quantification of Biocrusts. *Remote Sens.* **2019**, *11*, 1350. [CrossRef]

77. Rutherford, W.A.; Painter, T.H.; Ferrenberg, S.; Belnap, J.; Okin, G.O.; Flagg, C.; Reed, S.C. Albedo feedbacks to future climate via climate change impacts on dryland biocrusts. *Sci. Rep.* **2017**, *7*, 44188. [CrossRef]

78. Noy-Meir, I. Desert ecosystems: Environment and producers. *Annu. Rev. Ecol. Systemat.* **1973**, *4*, 25–51. [CrossRef]

79. Austin, A.T.; Yahdjian, L.; Stark, J.M.; Belnap, J.; Porporato, A.; Norton, U.; Ravetta, D.A.; Schaeffer, S.M. Water pulses and biogeochemical cycles in arid and semiarid ecosystems. *Oecologia* **2004**, *141*, 221–235. [CrossRef]

80. Ferrenberg, S.; Reed, S.C.; Belnap, J. Climate change and physical disturbance cause similar community shifts in biological soil crusts. *Proc. Natl. Acad. Sci. USA* **2015**, *112*, 12116–12121. [CrossRef]

81. Singer, M.J.; Le Bissonnais, Y. Importance of surface sealing in the erosion of some soils from a mediterranean climate. *Geomorphology* **1998**, *24*, 79–85. [CrossRef]

82. Malam Issa, O.; Cousin, I.; Le Bissonnais, Y.; Quétin, P. Dynamic evolution of the unsaturated hydraulic conductivity of a developing crust. *Earth Surf. Proc. Land* **2004**, *29*, 1131–1142. [CrossRef]

83. Neave, M.; Rayburg, S. A field investigation into the effects of progressive rainfall–induced soil seal and crust development on runoff and erosion rates: The impact of surface cover. *Geomorphology* **2007**, *87*, 378–390. [CrossRef]

84. Malam Issa, O.; Défarge, C.; Trichet, J.; Valentin, C.; Rajot, J.L. Microbiotic soil crusts in the Sahel of Western Niger and their influence on soil porosity and water dynamics. *Catena* **2009**, *77*, 48–55. [CrossRef]

85. Miralles-Mellado, I.; Cantón, Y.; Solé-Benet, A. Two-dimensional porosity of crusted silty soils: Indicators of soil quality in semiarid rangelands? *Soil Sci. Soc. Am. J.* **2011**, *75*, 1289–1301. [CrossRef]

86. Malam Issa, O.; Le Bissonnais, Y.; Défarge, C.; Trichet, J. Role of a microbial cover on structural stability of a sandy soil in Sahelian part of western Niger. *Geoderma* **2001**, *101*, 15–30. [CrossRef]

87. Rossi, F.; Potrafka, R.M.; Garcia Pichel, F.; De Philippis, R. The role of the exopolysaccharides in enhancing hydraulic conductivity of biological soil crusts. *Soil Biol. Biochem.* **2012**, *46*, 33–40. [CrossRef]

88. Román, J.R.; Roncero-Ramos, B.; Chamizo, S.; Rodríguez-Caballero, E.; Cantón, Y. Restoring soil functions by means of cyanobacteria inoculation: Importance of soil conditions and species selection. *Land Degrad. Dev.* **2018**, *29*, 3184–3193. [CrossRef]

89. Adessi, A.; Cruz de Carvalho, R.; De Philippis, R.; Branquinho, C.; Marques da Silva, J. Microbial extracellular polymeric substances improve water retention in dryland biological soil crusts. *Soil Biol. Biochem.* **2018**, *116*, 67–69. [CrossRef]

90. Kidron, G.J. Differential water distribution over dune slopes as affected by slope position and microbiotic crust, Negev Desert, Israel. *Hydrol. Process.* **1999**, *13*, 1665–1682. [CrossRef]

91. Fischer, T.; Veste, M.; Wiehe, W.; Lange, P. Water repellency and pore clogging at early successional stages of microbiotic crusts on inland dunes, Brandenburg, NE Germany. *Catena* **2010**, *80*, 47–52. [CrossRef]

92. Kidron, G.J.; Yaalon, D.H.; Vonshak, A. Two causes for runoff initiation on microbiotic crusts: Hydrophobicity and pore clogging. *Soil Sci.* **1999**, *164*, 18–27. [CrossRef]

93. Eldridge, D.J. Biological soil crusts and water relations in Australian deserts. In *Biological Soil Crusts: Structure, Function and Management*; Belnap, J., Lange, O.L., Eds.; Springer: Berlin/Heidelberg, Germany, 2003; pp. 119–131.

94. Zhang, J.; Zhang, Y.M.; Alison, D.; Cheng, J.H.; Zhou, X.B.; Zhang, B.C. The influence of biological soil crusts on dew deposition in Gurbantunggut Desert, Northwestern China. *J. Hydrol.* **2009**, *379*, 220–228. [CrossRef]

95. Pan, Y.X.; Wang, X.P.; Zhang, Y.F. Dew formation characteristics in a revegetation-stabilized desert ecosystem in Shapotou area, Northern China. *J. Hydrol.* **2010**, *387*, 265–272. [CrossRef]

96. Fischer, T.; Veste, M.; Bens, O.; Hüttl, R.F. Dew formation on the surface of biological soil crusts in central European sand ecosystems. *Biogeosciences* **2012**, *9*, 4621–4628. [CrossRef]

97. Colica, G.; Li, H.; Rossi, F.; Li, D.; Liu, Y.; De Philippis, R. Microbial secreted exopolysaccharides affect the hydrological behavior of induced biological soil crusts in desert sandy soils. *Soil Biol. Biochem.* **2014**, *68*, 62–70. [CrossRef]

98. Zangvil, A. Six years of dew observations in the Negev Desert, Israel. *J. Arid Environ.* **1996**, *32*, 361–371. [CrossRef]

99. Lange, O.L.; Kidron, G.J.; Büdel, B.; Meyer, A.; Kilian, E.; Abeliovich, A. Taxonomic composition and photosynthetic characteristics of the 'biological soil crusts' covering sand dunes in the western Negev Desert. *Funct. Ecol.* **1992**, *6*, 519–527. [CrossRef]

100. Cammeraat, L.H. Scale dependent thresholds in hydrological and erosion response of a semi-arid catchment in southeast Spain. *Agric. Ecosyst. Environ.* **2004**, *104*, 317–332. [CrossRef]

101. Martin, Y.; Valeo, C.; Tait, M. Centimetre-scale representations of terrain and impacts on depression storage and runoff. *Catena* **2008**, *75*, 223–233. [CrossRef]

102. Allmaras, R.R.; Burwell, R.E.; Larson, W.E.; Holt, R.F. Total porosity and random roughness of the interrow zone as influenced by tillage. *USDA Conserv. Res. Rep.* **1966**, *7*, 22.

103. Calvo-Cases, A.; Boix-Fayos, C.; Arnau-Rosalen, E. Patterns and thresholds of runoff generation and sediment transport on some Mediterranean hillslopes. In *Catchment dynamics and river processes: Mediterranean and other Climate Regions*; Garcia, C., Batalla, R.J., Eds.; Elsevier: San Diego, CA, USA, 2005; pp. 31–51.

104. Rodríguez-Caballero, E.; Castro, A.J.; Chamizo, S.; Quintas-Soriano, C.; Garcia-Llorente, M.; Cantón, Y.; Weber, B. Ecosystem services provided by biocrusts: From ecosystem functions to social values. *J. Arid. Environ.* **2018**, *159*, 45–53. [CrossRef]

105. Concostrina-Zubiri, L.; Huber-Sannwald, E.; Martínez, I.; Flores Flores, J.L.; Reyes-Agüero, J.A.; Escudero, A.; Belnap, J. Biological soil crusts across disturbance–recovery scenarios: Effect of grazing regime on community dynamics. *Ecol. Appl.* **2014**, *24*, 1863–1877. [CrossRef] [PubMed]

106. Mallen-Cooper, M.; Eldridge, D.J.; Delgado-Baquerizo, M. Livestock grazing and aridity reduce the functional diversity of biocrusts. *Plant Soil* **2018**, *429*, 175–185. [CrossRef]

107. Havrilla, C.A.; Chaudhary, V.B.; Ferrenberg, S.; Antoninka, A.J.; Belnap, J.; Bowker, M.A.; Eldridge, D.J.; Faist, A.M.; Huber-Sannwald, E.; Leslie, A.D.; et al. Towards a predictive framework for biocrust mediation of plant performance: A meta? *Anal. J. Ecol.* **2019**, *107*, 2789–2807. [CrossRef]

108. Zhao, Y.; Xu, M. Runoff and soil loss from revegetated grasslands in the Hilly Loess Plateau Region, China: Influence of biocrust patches and plant canopies. *J. Hydrol. Eng.* **2013**, *18*, 387–393. [CrossRef]

109. Li, X.J.; Li, X.R.; Song, M.; Gao, Y.P.; Zheng, J.G.; Jia, R.L. Effects of crust and shrub patches on runoff, sedimentation, and related nutrient (C, N) redistribution in the desertified steppe zone of the Tengger Desert, Northern China. *Geomorphology* **2008**, *96*, 221–232. [CrossRef]

110. Chamizo, S.; Rodríguez-Caballero, E.; Román, J.R.; Cantón, Y. Effects of biocrust on soil erosion and organic carbon losses under natural rainfall. *Catena* **2017**, *148*, 117–125. [CrossRef]

111. Thomas, A.D.; Dougill, A.J. Spatial and temporal distribution of cyanobacterial soil crusts in the Kalahari: Implications for soil surface properties. *Geomorphology* **2007**, *85*, 17–29. [CrossRef]

112. Svirčev, Z.; Dulić, T.; Obreht, I.; Codd, G.A.; Lehmkuhl, F.; Marković, S.B.; Hambach, U.; Meriluoto, J. Cyanobacteria and loess—An underestimated interaction. *Plant Soil* **2019**, *439*, 293–308.

113. Chen, L.; Sela, S.; Svoray, T.; Assouline, S. Scale dependence of Hortonian rainfall-runoff processes in a semiarid environment. *Water Resour. Res.* **2016**, *52*, 5149–5166. [CrossRef]

114. Rodríguez-Caballero, E.; Cantón, Y.; Jetten, V. Biological soil crust effects must be included to accurately model infiltration and erosion in drylands: An example from Tabernas Badlands. *Geomorphology* **2015**, *241*, 331–342. [CrossRef]

115. Lan, L.; Wu, L.; Zhang, D.; Hu, C. Assessing level of development and successional stages in biological soil crusts with biological indicators. *Microb. Ecol.* **2013**, *66*, 394–403. [CrossRef] [PubMed]